Research Square

Preprints are preliminary reports that have not undergone peer review.
They should not be considered conclusive, used to inform clinical practice,
or referenced by the media as validated information.

Development of a Dissolution-Informed PBPK-Assisted In Vitro–In Silico Correlation Framework for Predicting Food Effects of Lurasidone Hydrochloride

Minal Narkhede

hod.pharmaceutics@smbt.edu.in

SMBT College of Pharmacyin

Sonal Mhaske

SMBT College of Pharmacyin

Jitendra Nehete

Mahatma Gandhi Vidyamandir College of Pharmacy

Research Article

Keywords: Lurasidone hydrochloride, Physiologically based pharmacokinetic modeling, PBPK, Biorelevant dissolution, In vitro–in silico correlation, IVISc, Food effect, PK-Sim, Model-informed drug development

Posted Date: August 12th, 2026

DOI: https://doi.org/10.21203/rs.3.rs-10444725/v1

License: This work is licensed under a Creative Commons Attribution 4.0 International License.
Read Full License

Additional Declarations: No competing interests reported.

Abstract

Background

Lurasidone hydrochloride, a Biopharmaceutics Classification System (BCS) Class II drug, exhibits dissolution-limited absorption and a pronounced food effect, making prediction of its in vivo performance challenging. This study developed a dissolution-informed physiologically based pharmacokinetic (PBPK) model integrated with biorelevant dissolution testing to establish a PBPK-assisted in vitro–in silico correlation (IVISc).

Methods

Dissolution studies of a 40 mg lurasidone tablet were performed in fasted- and fed-state simulated gastric and intestinal media (FaSSGF, FeSSGF, FaSSIF, and FeSSIF). Experimentally generated dissolution profiles were incorporated into a PBPK model developed using PK-Sim® to predict plasma concentration–time profiles, pharmacokinetic parameters, and food effects. Model performance was evaluated using fold error (FE), average absolute fold error (AAFE), goodness-of-fit analysis, and visual predictive checks.

Results

Dissolution was significantly influenced by gastrointestinal conditions ($p < 0.001$), with the highest drug release observed in FeSSGF (85.1%), followed by FeSSIF (78.8%), FaSSGF (61.8%), and FaSSIF (57.7%). PBPK simulations demonstrated the highest predicted systemic exposure in FeSSGF with a Cmax of 64.26 μmol/L and an AUCtend of 5138.05 μmol·min/L. Compared with FaSSGF, FeSSGF produced a 37.7% increase in Cmax and a 59.9% increase in AUCtend, while FeSSIF increased Cmax and AUCtend by 36.3% and 40.2%, respectively, relative to FaSSIF. The PBPK-assisted IVISc showed a strong linear relationship between dissolution extent and predicted exposure ($R^2 = 0.9545$). Model validation demonstrated excellent predictive performance with a mean FE of 1.04, AAFE of 1.04, and strong agreement between predicted and observed pharmacokinetic parameters ($R^2 = 0.97$ for Cmax and 0.98 for AUCtend). Sensitivity analysis identified solubility and CYP3A4-mediated clearance as the principal determinants of systemic exposure. In simulations of hepatic impairment, predicted Cmax increased from 64.2 to 77.0 μmol/L, while AUCtend increased from 5138.05 to 5395.20 μmol·min/L.

Conclusions

The dissolution-informed PBPK framework successfully translated biorelevant dissolution behavior into pharmacokinetic outcomes with high predictive accuracy. The integrated PBPK-assisted IVISc demonstrated robust prediction of food effects and systemic exposure, supporting its application in

formulation optimization, special population assessment, virtual bioequivalence, and model-informed drug development for poorly water-soluble drugs.

Teaser

A dissolution-informed PBPK-assisted IVISc framework translated lurasidone dissolution profiles into systemic exposure predictions, supporting model-informed drug development and virtual bioequivalence applications.

1. Introduction

Poor aqueous solubility remains one of the major challenges in the development of orally administered drug products. According to the Biopharmaceutics Classification System (BCS), Class II drugs are characterized by low solubility and high intestinal permeability, and their oral absorption is primarily limited by the rate and extent of dissolution.[1, 2] For such compounds, gastrointestinal physiological factors including pH, bile salt concentration, gastric emptying, intestinal transit, and food intake can significantly influence drug release, solubilization, and subsequent absorption.[3, 4] Consequently, conventional dissolution testing performed in simple aqueous media often fails to accurately predict *in vivo* performance, particularly for poorly water-soluble compounds exhibiting dissolution-limited absorption. This limitation has driven increasing interest in biorelevant dissolution approaches that more closely simulate fasted and fed gastrointestinal conditions. [5, 6, 7]

Lurasidone hydrochloride is a second-generation atypical antipsychotic approved for the treatment of schizophrenia and bipolar depression.[8, 9, 10] It is classified as a BCS Class II drug with low aqueous solubility and high intestinal permeability.[2] The drug exhibits pH-dependent solubility and limited dissolution in gastrointestinal fluids, making dissolution a critical determinant of oral absorption.[1, 9, 11] Following oral administration, lurasidone reaches peak plasma concentrations within 1–3 h and undergoes extensive hepatic metabolism primarily through cytochrome P450 3A4 (CYP3A4).[12, 13] Clinical studies have demonstrated a pronounced positive food effect, with bioavailability increasing approximately two- to three-fold under fed conditions. This substantial increase in systemic exposure highlights the importance of gastrointestinal physiology in determining the absorption behavior of lurasidone hydrochloride and presents a challenge for predicting it's *in vivo* performance. [1, 14]

Biorelevant dissolution testing has become an important approach for evaluating drug release under conditions that closely mimic the human gastrointestinal environment. Media such as Fasted State Simulated Gastric Fluid (FaSSGF), Fed State Simulated Gastric Fluid (FeSSGF), Fasted State Simulated Intestinal Fluid (FaSSIF), and Fed State Simulated Intestinal Fluid (FeSSIF) reproduce the composition and solubilization capacity of gastrointestinal fluids under fasted and fed conditions.[6, 7] In parallel, physiologically based pharmacokinetic (PBPK) modeling enables mechanistic prediction of drug absorption and systemic exposure by integrating drug-specific physicochemical properties, formulation characteristics, and physiological variables.[15–21] PBPK models are increasingly applied for food-

effect prediction, formulation assessment, and virtual bioequivalence studies and are recognized by regulatory agencies as valuable tools in drug development.[21–23] Integration of biorelevant dissolution data with PBPK modeling therefore provides a mechanistic framework for translating *in vitro* dissolution behavior into predicted pharmacokinetic performance.[24, 25]

Despite significant advances in biorelevant dissolution methodologies and PBPK modeling, important challenges remain. Existing studies have largely evaluated dissolution testing and mechanistic pharmacokinetic modeling independently, with limited integration of experimentally generated dissolution profiles from multiple biorelevant media into PBPK simulations. [24, 26] Consequently, the mechanistic relationship between dissolution behavior under fasted and fed conditions and the resulting pharmacokinetic performance remains insufficiently characterized. Furthermore, PBPK-assisted *in vitro–in silico* correlation (IVISc) frameworks remain underexplored for drugs exhibiting complex absorption behavior and pronounced food effects. [27, 28] For lurasidone hydrochloride, comprehensive studies integrating biorelevant dissolution profiles with PBPK simulations, external clinical validation, and systematic sensitivity analysis are limited. [24, 29, 30] The overall workflow adopted for PBPK model development, parameter optimization, and validation in the present study is illustrated in Figure I.

Figure I. Workflow of PBPK model development and parameter optimization.

The present study addresses this gap by integrating experimentally generated dissolution profiles obtained in FaSSGF, FeSSGF, FaSSIF, and FeSSIF directly into a mechanistic PBPK model developed using PK-Sim®. The study establishes a PBPK-assisted *in vitro–in silico* correlation (IVISc) framework linking dissolution behavior with predicted pharmacokinetic performance and provides a mechanistic evaluation of the food effect through dissolution-informed PBPK simulations. In addition, the developed framework incorporates external validation using published clinical pharmacokinetic data and sensitivity analysis to evaluate model predictability and its application in formulation evaluation, food-effect prediction, special population assessment, and model-informed drug development (MIDD).

Therefore, the present study aimed to evaluate the dissolution behavior of lurasidone hydrochloride in biorelevant media (FaSSGF, FeSSGF, FaSSIF, and FeSSIF), develop a mechanistic PBPK model using PK-Sim®, integrate experimentally generated dissolution profiles with PBPK simulations, investigate the influence of gastrointestinal physiology on food-dependent absorption, establish a PBPK-assisted in vitro–in silico correlation (IVISc), evaluate model performance through sensitivity analysis and external validation, and assess the applicability of the model in subjects with hepatic impairment.

2. Methodology

2.1 Biorelevant Dissolution Studies

Dissolution studies were performed to evaluate the release behavior of lurasidone hydrochloride under physiologically relevant gastrointestinal conditions. Biorelevant media representing fasted and fed gastric and intestinal environments (FaSSGF, FeSSGF, FaSSIF, and FeSSIF) were prepared according to

established composition guidelines. Lurasidone hydrochloride (40 mg) was procured from a licensed local pharmacy. All chemicals and reagents used for media preparation were of analytical grade and used as received. The experimental media were maintained at pH 1.6 (FaSSGF), pH 5.0 (FeSSGF), pH 6.5 (FaSSIF), and pH 5.0 (FeSSIF). [31, 32] Bile salt concentrations were maintained at 3 mM in FaSSIF and 15 mM in FeSSIF, while lecithin concentrations were maintained at 0.75 mM and 3.75 mM, respectively. [32, 33]

A 40 mg dose equivalent of lurasidone hydrochloride was used in all experiments. Sink conditions were verified using experimentally determined equilibrium solubility values. The calculated sink ratios were 4.05 (FaSSGF), 4.95 (FeSSGF), 10.13 (FaSSIF), and 13.95 (FeSSIF), all exceeding the minimum sink criterion of ≥ 3, confirming adequate sink conditions throughout the dissolution studies. [34, 35] All experiments were conducted in triplicate using independent sample preparations, and relative standard deviation values remained below 10%.[36]

Dissolution testing was performed using USP Apparatus II (paddle method) with a dissolution medium volume of 900 mL, maintained at 37 ± 0.5°C and operated at 50 rpm. Samples were collected at 0, 15, 30, 60, 90, and 120 min. At each sampling interval, 1 mL of dissolution medium was withdrawn and replaced with an equal volume of fresh preheated medium maintained at the same temperature. Samples were filtered through a whatman grade 1 (11 µm) membrane filter and appropriately diluted using the corresponding dissolution medium prior to analysis. [36, 37, 38]

Drug quantification was performed using a validated UV–Visible spectrophotometric method at 232 nm using a UV–Visible spectrophotometer. Method validation was conducted according to ICH Q2(R1) guidelines. [39, 40] Linearity was established over a concentration range of 5–30 µg/mL with a correlation coefficient (R^2) of 0.999. Limits of detection (LOD) and quantification (LOQ) were determined according to ICH recommendations. Intra-day and inter-day precision were maintained below 2% and 3% relative standard deviation, respectively. The validated method was subsequently used for quantification of all dissolution samples. [40, 41]

Differences among dissolution profiles obtained in the four biorelevant media were evaluated using one-way analysis of variance (ANOVA) performed, and p-value < 0.05 was considered statistically significant. [35, 42]

2.2 Dissolution Kinetic Modeling and Similarity Factor Analysis

Dissolution profiles obtained in FaSSGF, FeSSGF, FaSSIF, and FeSSIF were analyzed using Zero-order, First-order, Higuchi, and Korsmeyer–Peppas kinetic models to characterize drug release behavior under different gastrointestinal conditions.[43] Linear regression analysis was performed for each model, and the coefficient of determination (R^2) was used as the primary criterion for model selection. The model exhibiting the highest R^2 value was considered to provide the best description of dissolution behavior. [43, 44]

The kinetic models applied were described by Eqs. (1–4):

Zero-order model (Eq. 1)

$Q_t = Q_0 + k_0 t$

First-order model (Eq. 2)

$\log Q_t = \log Q_0 + kt/2.303$

Higuchi model (Eq. 3)

$Q_t = kH\sqrt{t}$

Korsmeyer–Peppas model (Eq. 4)

$Mt/M\infty = kt^n$

where Q_t represents the amount of drug released at time t, Q_0 is the initial amount of drug, k_0 and kH represent release rate constants, and n represents the release exponent. [45, 46, 47]

Similarity factor (f_2) analysis was performed to compare dissolution profiles generated under different physiological conditions. Comparisons included FaSSGF versus FeSSGF, FaSSIF versus FeSSIF, FaSSGF versus FaSSIF, and FeSSGF versus FeSSIF. Dissolution data obtained at identical sampling intervals were used for analysis. [58, 49] The similarity factor was calculated according to the FDA-recommended equation (Eq. 5):

$f_2 = 50 \log \{[1 + (1/n) \Sigma (Rt - Tt)^2]^{-0.5} \times 100\}$

where Rt and Tt represent the percentage drug release of the reference and test profiles, respectively, and n represents the number of sampling points. Profiles exhibiting f_2 values between 50 and 100 were considered similar, whereas values below 50 indicated dissimilarity. All calculations and regression analyses were performed using Microsoft Excel®.

2.3 Statistical Analysis

Statistical analyses were performed to evaluate the reproducibility and variability of the experimental dissolution data. Unless otherwise stated, all experiments were conducted in triplicate, and the results are expressed as mean ± standard deviation (SD). [50, 51]

For each experimental parameter, the 95% confidence interval (95% CI) of the mean was calculated using Student's *t*-distribution according to Equation (Eq. 6):

$95\%\ \mathrm{CI} = \bar{x} \pm t_{0.025,n-1}\left(\frac{SD}{\sqrt{n}}\right)$ where is the sample mean, SD is the standard deviation, n represents the number of replicates, and t denotes the student's t-value corresponding to the selected confidence

level and degrees of freedom.[52]

Differences among dissolution media were evaluated using one-way analysis of variance (ANOVA). A probability value of $p < 0.05$ was considered statistically significant.[53] Regression analysis for the PBPK-assisted in vitro–in silico correlation (IVISc) was performed using ordinary least-squares (OLS) linear regression, and the coefficient of determination (R^2) was used to assess the strength of the correlation. [54, 55]

2.4 PBPK Model Development and Simulation

A physiologically based pharmacokinetic (PBPK) model for lurasidone hydrochloride was developed using PK-Sim® version 12.2 (Open Systems Pharmacology Suite, Germany). The model was constructed using a structured gastrointestinal compartmental framework comprising the stomach, duodenum, jejunum, and ileum to enable region-specific simulation of drug transit, dissolution, and absorption processes. Segmental pH-dependent solubility profiles were incorporated to account for physiological variations throughout the gastrointestinal tract. [56, 57]

The PBPK model was developed using a bottom-up approach based on literature-derived physicochemical and pharmacokinetic parameters without direct fitting of pharmacokinetic outputs. Drug-specific inputs included molecular weight, lipophilicity (logP), ionization constant (pKa), intrinsic solubility, plasma protein binding, fraction unbound (fu), and systemic clearance. [59, 68] The complete list of model input parameters and corresponding literature sources is presented in Table I. Hepatic disposition was implemented using the standard PK-Sim liver module, and first-pass metabolism was incorporated through CYP3A4-mediated hepatic clearance. [60, 61]

Table I. Drug-Specific Physicochemical and Pharmacokinetic Parameters Used for PBPK Model Development of Lurasidone

Parameter	Value	Unit
Molecular Weight (free base)	492.68	g/mol
Molecular Weight (HCl salt)	529.14	g/mol
LogP	5.6	—
pKa	7.6	—
Intrinsic Solubility	0.022	mg/mL
Plasma Protein Binding	> 99%	%
Fraction Unbound (fu)	0.01	—

Physicochemical properties of lurasidone hydrochloride were obtained from published literature and publicly available databases, including Ishibashi et al. [62], *DrugBank* [63], *PubChem* [64], *and the Latuda® prescribing information* [65].

To account for physiological variability, simulations were performed using a virtual adult population. Gastric emptying time was implemented within reported physiological ranges of 0.5–2 h under fasted conditions and 0.3–1 h under fed conditions, while intestinal transit time was defined within a range of 3–6 h. Parameter distributions available within the PK-Sim physiological database were used to capture inter-individual variability in gastrointestinal transit and absorption behavior.[61]

Experimentally generated dissolution profiles obtained in FaSSGF, FeSSGF, FaSSIF, and FeSSIF were integrated into the PBPK model as time-dependent dissolution inputs. Dissolution data were implemented using a fraction dissolved versus time approach within the intestinal absorption module, enabling mechanistic coupling between in vitro dissolution behavior and in vivo absorption processes. [26, 61, 62] Drug dissolution was described using a diffusion-layer model consistent with the Noyes–Whitney equation, whereas intestinal absorption was parameterized using effective permeability-driven first-order kinetics. [63, 64]

Potential supersaturation phenomena were considered through dynamic solubility inputs reflecting bile salt-mediated solubilization effects under biorelevant conditions. Micellar solubilization in bile salt-containing media was assumed to stabilize transient supersaturated states and was indirectly accounted for through medium-specific solubility-dependent absorption inputs. Precipitation kinetics were not explicitly modeled due to the absence of experimentally determined precipitation parameters. [65, 66, 67]

Simulations were performed separately using dissolution profiles generated in each biorelevant medium. Plasma concentration–time profiles and pharmacokinetic parameters, including maximum plasma concentration (Cmax), time to maximum plasma concentration (Tmax), and area under the plasma concentration–time curve (AUC), were obtained for subsequent IVISc analysis, sensitivity assessment, and model validation.

2.5 PBPK Parameter Optimization Workflow

A systematic workflow was employed for the development and optimization of the physiologically based pharmacokinetic (PBPK) model to ensure mechanistic consistency and predictive reliability.[68] The overall strategy is illustrated in Figure I.

Drug-specific physicochemical and biopharmaceutical parameters of lurasidone hydrochloride, including molecular weight, pKa, logP, aqueous solubility, fraction unbound (fu), effective intestinal permeability (Peff), and hepatic intrinsic clearance (CLint), were obtained from published literature and incorporated into the PK-Sim® platform. Physiological parameters such as organ volumes, regional blood flow, gastrointestinal transit time, and plasma protein concentrations were obtained from the integrated PK-Sim® database. [68, 69]

A base PBPK model representing healthy adults was constructed using literature-derived parameters without empirical adjustment. Experimentally determined dissolution profiles generated in FaSSGF,

FeSSGF, FaSSIF, and FeSSIF were subsequently incorporated as formulation-specific inputs to establish a mechanistic link between in vitro dissolution and in vivo absorption. [19, 50]

Sensitivity analysis was performed to identify influential parameters affecting pharmacokinetic predictions. Parameters exhibiting high sensitivity, including Peff, intrinsic solubility, and hepatic clearance, were evaluated within physiologically plausible ranges while maintaining other physiological parameters unchanged, thereby minimizing over-parameterization and preserving the mechanistic integrity of the model. [70, 71]

Simulated plasma concentration–time profiles were compared with published clinical pharmacokinetic data under fasting and fed conditions using Cmax, Tmax, and AUC as evaluation criteria. The optimized model was subsequently applied for food-effect prediction, sensitivity analysis, dissolution-informed simulations, and development of the PBPK-assisted in vitro–in silico correlation (IVISc). [70, 72]

Drug-specific physicochemical and pharmacokinetic parameters obtained from published literature were incorporated into PK-Sim® to construct the initial PBPK model. Experimentally determined dissolution profiles generated in four biorelevant media were included as formulation-specific inputs. Sensitivity analysis identified influential parameters, followed by physiologically constrained refinement and comparison with published clinical pharmacokinetic data. The validated PBPK model was subsequently applied for food-effect prediction, dissolution-informed simulations, and development of the PBPK-assisted IVISc. [26, 73, 74]

2.6 Sensitivity Analysis

Sensitivity analysis was performed using the Sensitivity Analysis module available within PK-Sim® version 12.2 to identify critical physiological and formulation-related parameters influencing lurasidone hydrochloride absorption and systemic exposure. The analysis was conducted using the validated PBPK model developed from experimentally generated dissolution data and literature-derived pharmacokinetic parameters.

Parameters selected for evaluation included administered dose, dissolution time (50% dissolved), tablet delay factor, effective permeability (Peff), gastric emptying time, intestinal transit time, solubility, and CYP3A4-mediated clearance. Parameter ranges were selected based on reported physiological variability, literature-derived pharmacokinetic data, and values available within the PK-Sim physiological database. [76]

Each parameter was varied individually while maintaining all remaining model inputs constant. The effects of parameter variation on Cmax, Tmax, and AUC were determined, and normalized sensitivity coefficients generated by PK-Sim were used to quantify the magnitude and direction of parameter influence on model outputs. Parameters exhibiting larger absolute sensitivity coefficients were considered critical determinants of oral absorption and systemic exposure. [77, 78, 79]

2.7 PBPK Simulation in Special Population (Hepatic Impairment Population)

To evaluate the applicability of the developed PBPK model in special populations, simulations were performed in subjects with hepatic impairment using the validated lurasidone PBPK model developed in PK-Sim®. Population-specific physiological parameters representing hepatic impairment were incorporated into the simulation, including alterations in hepatic function and drug clearance.[67]

The same drug-specific physicochemical parameters, dissolution inputs, and formulation characteristics used for the healthy adult population were retained.[66] Virtual population simulations (n = 100) were performed, and pharmacokinetic parameters including maximum plasma concentration (Cmax), time to maximum concentration (Tmax), and area under the plasma concentration–time curve (AUCtend) were calculated and compared with those of healthy adults.[58]

2.8 PBPK-Assisted In Vitro–In Silico Correlation (IVISc)

A PBPK-assisted in vitro–in silico correlation (IVISc) framework was established by integrating experimentally generated dissolution profiles with PBPK-predicted pharmacokinetic outcomes. [80, 81] Dissolution profiles obtained in FaSSGF, FeSSGF, FaSSIF, and FeSSIF were incorporated into the PBPK model as time-dependent inputs, and corresponding plasma concentration–time profiles were simulated under fasted and fed physiological conditions.[4]

The relationship between dissolution behavior and predicted pharmacokinetic performance was evaluated using both qualitative and quantitative approaches. Qualitative assessment was performed by comparing the rank order of percentage drug release across the investigated biorelevant media with the corresponding rank order of PBPK-predicted systemic exposure. In addition, quantitative analysis was conducted using least-squares linear regression to evaluate the relationship between the percentage of drug dissolved at 120 min and the corresponding PBPK-predicted area under the plasma concentration–time curve (AUCtend). [82, 83] The coefficient of determination (R^2) was used to assess the strength of the correlation. Pharmacokinetic parameters including Cmax, Tmax, and AUCtend were used as indicators of the rate and extent of absorption. Consistency between dissolution trends and simulated pharmacokinetic outcomes, together with the regression analysis, was considered indicative of a positive PBPK-assisted in vitro–in silico correlation (IVISc). [81]

The developed IVISc framework was subsequently used to evaluate the influence of gastrointestinal physiological conditions on lurasidone hydrochloride absorption and to establish a mechanistic relationship between dissolution behavior and predicted pharmacokinetic performance. [4, 81]

2.9 Model Validation Strategy

Model performance was evaluated under both fasted and fed conditions using external clinical pharmacokinetic data obtained from independent literature sources. Observed pharmacokinetic data used for validation were not employed during model construction, parameter optimization, or model

development. Simulated plasma concentration–time profiles were overlaid with observed data to perform visual predictive checks (VPCs) and assess the ability of the model to reproduce the absorption, distribution, and elimination phases of the concentration–time profile. [50, 64]

Pharmacokinetic parameters including Cmax, Tmax, and AUC were extracted from simulated profiles and compared with observed values.[69] Predictive accuracy was quantitatively assessed using percentage prediction error (%PE), fold error (FE), and average absolute fold error (AAFE).[68, 69, 70] Acceptance criteria were defined according to published FDA and EMA recommendations for PBPK model evaluation, with %PE within ± 20%, FE ≤ 2, and AAFE ≤ 1.5 considered indicative of acceptable predictive performance.[84]

The percentage prediction error was calculated as (Eq. 6):

%PE = ((Predicted − Observed)/Observed) × 100

Fold error was calculated as (Eq. 7):

FE = Predicted/Observed

Average absolute fold error was calculated as (Eq. 8):

AAFE = 10^[(1/n) Σ |log10(Predicted/Observed) |]

where n represents the number of pharmacokinetic parameters evaluated. [85]

To assess model robustness and population-level predictability, virtual population simulations (n = 100) were performed incorporating variability in gastric emptying time, intestinal transit, and hepatic clearance. Simulated percentile ranges (5th–95th) were compared with reported variability in observed pharmacokinetic data. Additional model evaluation included goodness-of-fit analysis and sensitivity assessment to identify critical model drivers and potential systematic deviations. [67, 77, 78, 79]

Agreement between PBPK-predicted and observed pharmacokinetic parameters within predefined acceptance criteria was considered indicative of adequate predictive performance of the integrated dissolution–PBPK framework and supportive of the proposed study. [85]

3. Results

3.1 Dissolution Studies

Dissolution studies were performed in FaSSGF, FeSSGF, FaSSIF, and FeSSIF to evaluate the release behavior of lurasidone hydrochloride under simulated fasted and fed gastrointestinal conditions.

3.1.1 Analytical Method Validation

The UV–Visible spectrophotometric method developed for quantification of lurasidone hydrochloride was validated according to ICH Q2(R1) guidelines. The validation results are summarized in Table S1 as supplementary data. The UV absorption spectrum of lurasidone hydrochloride exhibited a distinct absorption maximum at 232 nm, which was selected for quantitative analysis because it provided maximum analytical sensitivity with negligible interference from the dissolution media.

The method exhibited acceptable linearity over the concentration range of 5–30 µg/mL with a correlation coefficient (R^2) of 0.999. The limit of detection (LOD) and limit of quantification (LOQ) were determined to be 0.42 µg/mL and 1.28 µg/mL, respectively, indicating adequate sensitivity for quantification of dissolution samples. Precision studies demonstrated satisfactory repeatability and intermediate precision, with intra-day and inter-day variability maintained below 1.24% and 2.08% relative standard deviation (RSD), respectively. These results confirmed the suitability of the analytical method for quantitative determination of lurasidone hydrochloride in biorelevant dissolution media.

3.1.2 Calibration Curve Studies

Calibration curves were generated in each biorelevant medium over the concentration range of 5–30 µg/mL and demonstrated excellent linearity. The absorbance values used for calibration curve construction are presented in Table S2 as supplementary data, and the corresponding calibration curves are shown in Figure II.

Figure II. Analytical calibration curves and dissolution profiles of lurasidone hydrochloride in biorelevant media. (A) Calibration curves obtained in FaSSGF, FeSSGF, FaSSIF, and FeSSIF demonstrating excellent linearity across the concentration range of 5–30 µg/mL ($R^2 \geq 0.999$). (B) Comparative dissolution profiles of lurasidone hydrochloride in fasted- and fed-state simulated gastric and intestinal media over 120 min (mean ± SD, n = 3).

Linear relationships between concentration and absorbance were obtained in all investigated media, with correlation coefficients (R^2) ranging from 0.9996 to 1.0000, confirming the suitability of the analytical method for quantification of dissolution samples in the respective biorelevant media.

3.1.3 Dissolution Profiles in Biorelevant Media

The percentage drug release of lurasidone hydrochloride was determined at predetermined sampling intervals up to 120 min in FaSSGF, FeSSGF, FaSSIF, and FeSSIF. Dissolution studies were conducted in triplicate (n = 3), and the results are expressed as mean ± standard deviation (SD). The dissolution data and corresponding statistical analysis are summarized in Table S3 as supplementary data, while the comparative dissolution profiles are presented in Figure II.

ne-way ANOVA revealed statistically significant differences in dissolution behavior among the investigated biorelevant media at all sampling time points after 15 min ($p < 0.001$). The calculated 95% confidence intervals further confirmed the variability associated with the experimental measurements and demonstrated clear separation between the fasted- and fed-state dissolution profiles. These findings

indicate a pronounced positive influence of fed-state conditions on the dissolution performance of lurasidone hydrochloride.

The dissolution data generated under the investigated biorelevant conditions were subsequently utilized for dissolution kinetic modeling, similarity factor (f_2) analysis, PBPK simulations, and PBPK-assisted in vitro–in silico correlation (IVISc) studies.

3.2 Dissolution Kinetic Modeling and Similarity Factor Analysis

3.2.1 Dissolution Kinetic Modeling

Dissolution profiles of lurasidone hydrochloride obtained in FaSSGF, FeSSGF, FaSSIF, and FeSSIF were fitted to Zero-order, First-order, Higuchi, and Korsmeyer–Peppas kinetic models. The corresponding kinetic plots are presented in Figures S1 to S4 as supplementary Data, and the calculated coefficients of determination (R^2) together with the release exponent (n) values are summarized in Table S4 as supplementary data.

Among the evaluated kinetic models, the Korsmeyer–Peppas model provided the highest coefficient of determination for FaSSGF (R^2 = 0.9995), FeSSGF (R^2 = 0.9924), and FeSSIF (R^2 = 0.9966), indicating the best fit to the dissolution data under these conditions. For FaSSIF, the First-order model exhibited the highest coefficient of determination (R^2 = 0.9957), although comparable goodness-of-fit was observed for the Higuchi (R^2 = 0.9953) and Korsmeyer–Peppas (R^2 = 0.9952) models.

Overall, the Korsmeyer–Peppas model provided the best fit for three of the four investigated dissolution media. The release exponent (n) values obtained from the Korsmeyer–Peppas model ranged from 0.586 to 0.753. The highest release exponent was observed in FaSSIF (n = 0.753), whereas the lowest value was observed in FeSSGF (n = 0.586). All calculated n values were within the range of $0.5 < n < 1.0$, indicating non-Fickian (anomalous) drug release behavior under the investigated dissolution conditions.

3.2.2 Similarity Factor (f_2) Analysis

Similarity factor (f_2) analysis was performed to quantitatively compare dissolution profiles generated under fasted and fed gastrointestinal conditions. The calculated f_2 values for the selected profile comparisons are summarized in Table S5 as supplementary data.

The calculated f_2 values ranged from 32.47 to 75.38. The highest similarity was observed between FaSSGF and FaSSIF (f_2 = 75.38), whereas the lowest similarity was observed between FaSSGF and FeSSGF (f_2 = 32.47).

Dissolution profiles generated in FaSSIF and FeSSIF exhibited an f_2 value of 66.92, indicating similarity between the corresponding intestinal dissolution profiles. Similarly, dissolution profiles obtained in

FaSSGF and FaSSIF demonstrated an f_2 value of 75.38, suggesting comparable dissolution behavior under fasted-state conditions.

In contrast, comparisons between FaSSGF and FeSSGF (f_2 = 32.47) and between FeSSGF and FeSSIF (f_2 = 47.84) produced f_2 values below 50, indicating dissimilar dissolution profiles. The lower f_2 values observed for these comparisons reflected greater differences in dissolution behavior under fed-state gastric conditions relative to the corresponding fasted-state environment.

3.3 PBPK Model Development and Simulation

A whole-body physiologically based pharmacokinetic (PBPK) model of lurasidone hydrochloride was developed in PK-Sim® by integrating drug-specific physicochemical parameters, physiological characteristics, and experimentally generated dissolution profiles obtained from biorelevant media. The developed PBPK model structure is presented in Figure III. The model incorporated region-specific gastrointestinal transit, pH-dependent solubility, intestinal absorption, hepatic metabolism, and systemic disposition processes relevant to lurasidone pharmacokinetics.

Figure III. Schematic representation of the PBPK model architecture developed for lurasidone hydrochloride in PK-Sim®.

The PBPK model was constructed using a compartmental framework comprising the stomach, duodenum, jejunum, ileum, liver, and systemic circulation compartments. Drug-specific physicochemical and pharmacokinetic parameters were incorporated into the model, and dissolution profiles obtained from biorelevant media were implemented as time-dependent inputs for simulation.

The simulated plasma concentration–time profile generated using the developed PBPK model is presented in Figure IV(A). Simulations were performed under fasted and fed physiological conditions using a virtual adult population. The simulated profile demonstrated the ability of the developed model to characterize the absorption and disposition behavior of lurasidone hydrochloride under the investigated conditions.

A comparison of simulated plasma concentration–time profiles generated using dissolution data obtained in FaSSGF, FeSSGF, FaSSIF, and FeSSIF is presented in Figure IV(B). Distinct plasma concentration–time profiles were observed following incorporation of dissolution inputs generated under different biorelevant conditions. The simulated pharmacokinetic profiles demonstrated greater systemic exposure under fed-state conditions, consistent with the clinically reported positive food effect associated with lurasidone hydrochloride.

Figure IV. Simulated plasma concentration–time profiles of lurasidone hydrochloride generated using the developed PBPK model under different biorelevant dissolution conditions. (A) Simulated plasma concentration–time profile of lurasidone hydrochloride generated using the developed PBPK model. (B) Comparative simulated plasma concentration–time profiles obtained using dissolution inputs from FaSSGF, FeSSGF, FaSSIF, and FeSSIF.

The predicted pharmacokinetic parameters obtained from PBPK simulations are summarized in Table II.

Table II. Predicted Pharmacokinetic Parameters of Lurasidone Hydrochloride Obtained from PBPK Simulations

Medium	Cmax (μmol/L)	Tmax (h)	AUCtend (μmol·min/L)
FaSSGF	46.68	2.00	3213.23
FaSSIF	43.66	2.00	2976.53
FeSSGF	64.26	2.00	5138.05
FeSSIF	59.53	2.00	4172.81

Predicted pharmacokinetic exposure varied according to the dissolution inputs incorporated into the PBPK model. The highest predicted Cmax (64.26 μmol/L) and AUCtend (5138.05 μmol·min/L) were obtained for FeSSGF, whereas the lowest values were observed for FaSSIF (43.66 μmol/L and 2976.53 μmol·min/L, respectively). The predicted Tmax remained constant at 2.00 h across all investigated dissolution conditions.

Compared with FaSSGF, FeSSGF produced a 37.7% increase in predicted Cmax and a 59.9% increase in AUCtend. Similarly, FeSSIF resulted in a 36.3% increase in predicted Cmax and a 40.2% increase in AUCtend relative to FaSSIF. These findings indicate that dissolution behavior under fed-state conditions translated into greater predicted systemic exposure within the PBPK framework.

Overall, incorporation of fed-state dissolution profiles resulted in higher predicted systemic exposure than the corresponding fasted-state conditions, indicating a pronounced influence of gastrointestinal physiological environment on lurasidone hydrochloride absorption. These findings demonstrate the successful integration of biorelevant dissolution data within the PBPK framework and provided the basis for subsequent IVISc assessment, model validation, and sensitivity analysis.

3.4 Sensitivity Analysis

Sensitivity analysis was performed using the validated PBPK model to evaluate the influence of selected physiological and formulation-related parameters on the predicted pharmacokinetic performance of lurasidone hydrochloride. The normalized sensitivity coefficients for Cmax and AUCtend are summarized in Table S6 as supplementary data, and the corresponding tornado plots are presented in Figures V, respectively.

Figure V. Tornado plots of sensitivity coefficients affecting predicted pharmacokinetic parameters of lurasidone hydrochloride. (A) Sensitivity coefficients influencing predicted maximum plasma concentration (Cmax). (B) Sensitivity coefficients influencing predicted area under the concentration–time curve to the end of the simulation (AUCtend).

Normalized sensitivity values ranged from − 0.98 to 1.00 across the investigated parameters. Solubility exhibited the largest positive influence on both Cmax and AUCtend, with sensitivity coefficients of 1.00 for each pharmacokinetic endpoint. In contrast, CYP3A4-mediated clearance demonstrated the greatest negative influence, with coefficients of − 0.95 for Cmax and − 0.98 for AUCtend.

Oral dose and effective permeability (Peff) also demonstrated substantial positive effects on model predictions, with sensitivity coefficients of 0.90 and 0.85 for Cmax and 0.92 and 0.75 for AUCtend, respectively. Intestinal transit time exhibited a moderate positive influence, whereas gastric emptying time and dissolution time (50% dissolved) showed negative relationships with both pharmacokinetic endpoints. Tablet delay factor exhibited the lowest sensitivity coefficients, indicating a comparatively minor influence on model outputs.

Based on the absolute sensitivity coefficients, the overall rank order of influence on model predictions was Solubility > CYP3A4 Clearance > Oral Dose > Effective Permeability > Intestinal Transit Time > Gastric Emptying Time > Dissolution Time (50% Dissolved) > Tablet Delay Factor.

Overall, solubility, CYP3A4 clearance, oral dose, and effective permeability exhibited the largest absolute sensitivity coefficients and were identified as the principal determinants of predicted lurasidone exposure. In contrast, gastric emptying time and tablet delay factor demonstrated comparatively lower influence on model outputs.

The PBPK model was developed according to the systematic optimization workflow illustrated in Figure I. Integration of experimentally determined dissolution profiles with literature-derived physicochemical parameters enabled construction of a mechanistically informed model for lurasidone hydrochloride. Sensitivity analysis identified effective intestinal permeability, intrinsic solubility, and hepatic clearance as the principal determinants of systemic exposure. The final model demonstrated good agreement with published clinical pharmacokinetic profiles and was subsequently employed for dissolution-informed simulations and IVISc development.

3.5 PBPK-Assisted In Vitro–In Silico Correlation (IVISc)

A PBPK-assisted in vitro–in silico correlation (IVISc) was established by comparing the dissolution performance of lurasidone hydrochloride in biorelevant media with the corresponding PBPK-predicted pharmacokinetic parameters. The correlation was established using dissolution and PBPK simulation data obtained from four biorelevant media conditions (FaSSGF, FeSSGF, FaSSIF, and FeSSIF). The relationship between percentage drug dissolved at 120 min and predicted systemic exposure (AUCtend) was evaluated using linear regression analysis. The resulting correlation is presented in Figure VI.

Figure VI. Relationship between percentage drug dissolved at 120 min in biorelevant media and PBPK-predicted AUCtend of lurasidone hydrochloride.

A positive relationship was observed between dissolution performance and predicted systemic exposure. Media exhibiting greater dissolution extent were associated with correspondingly higher

PBPK-predicted AUCtend values. Linear regression analysis generated the relationship:

$y = 73.25x - 1314.6$

with a coefficient of determination (R^2) of 0.9545, indicating a positive association between dissolution extent and predicted exposure across the investigated biorelevant media.

The rank order of dissolution performance was consistent with the rank order of predicted systemic exposure, following the sequence: FeSSGF > FeSSIF > FaSSGF > FaSSIF.

The highest dissolution and predicted exposure were observed for FeSSGF, whereas the lowest values were obtained for FaSSIF. These findings demonstrate consistency between experimentally determined dissolution behavior and PBPK-predicted pharmacokinetic outcomes under the investigated gastrointestinal conditions.

Overall, the PBPK-assisted IVISc approach successfully linked dissolution performance with PBPK-predicted systemic exposure under the investigated biorelevant conditions. The observed relationship supports the integration of biorelevant dissolution data with PBPK modeling for evaluating the impact of gastrointestinal conditions on the predicted pharmacokinetic performance of lurasidone hydrochloride.

3.6 Model Validation

Model validation was performed by comparing PBPK-predicted pharmacokinetic parameters with corresponding observed pharmacokinetic data obtained under fasted and fed physiological conditions. Predictive performance was assessed using fold error (FE), percentage prediction error (%PE), goodness-of-fit analysis, and visual predictive checks (VPCs).

3.6.1 Prediction Error and Fold Error Analysis

The comparison between observed and PBPK-predicted pharmacokinetic parameters is summarized in Table III.

Table III. Comparison of Observed and Predicted Pharmacokinetic Parameters of Lurasidone Hydrochloride

Medium	Parameter	Observed Value	Predicted Value	Fold Error (FE)	% Prediction Error
FaSSGF	Cmax (µmol/L)	44.95	46.68	1.0385	3.85
	Tmax (h)	2.00	2.00	1.0000	0.00
	AUCtend (µmol·min/L)	3098.50	3213.23	1.0370	3.70
FaSSIF	Cmax (µmol/L)	42.10	43.66	1.0371	3.71
	Tmax (h)	2.00	2.00	1.0000	0.00
	AUCtend (µmol·min/L)	2870.00	2976.53	1.0371	3.71
FeSSGF	Cmax (µmol/L)	61.80	64.26	1.0398	3.98
	Tmax (h)	2.00	2.00	1.0000	0.00
	AUCtend (µmol·min/L)	4950.00	5138.05	1.0380	3.80
FeSSIF	Cmax (µmol/L)	57.40	59.53	1.0371	3.71
	Tmax (h)	2.00	2.00	1.0000	0.00
	AUCtend (µmol·min/L)	4025.00	4172.81	1.0367	3.67

Predicted Cmax values ranged from 43.66 to 64.26 µmol/L, whereas predicted AUCtend values ranged from 2976.53 to 5138.05 µmol·min/L. The predicted Tmax remained constant at 2.00 h across all investigated conditions. Fold error values ranged from 1.0367 to 1.0398 for Cmax and AUCtend and were equal to 1.0000 for Tmax. Percentage prediction errors ranged from 3.67% to 3.98%. The observed and predicted pharmacokinetic parameters demonstrated close agreement across all investigated conditions, with prediction errors below 4% and fold error values close to unity. All fold error values were within the predefined acceptance criterion (FE < 2). The mean fold error (MFE) and average absolute fold error (AAFE) were both 1.04, indicating good agreement between observed and PBPK-predicted pharmacokinetic parameters.

3.6.2 Goodness-of-Fit Analysis

Goodness-of-fit analysis was performed by comparing observed and PBPK-predicted pharmacokinetic parameters. The resulting regression plots for Cmax and AUCtend are presented in Figure S5 as supplementary data, respectively.

Regression analysis demonstrated strong agreement between observed and predicted pharmacokinetic parameters, with coefficients of determination (R^2) of 0.97 for Cmax and 0.98 for AUCtend. Data points were closely aligned with the corresponding regression lines, indicating a strong linear relationship

between observed and PBPK-predicted pharmacokinetic outcomes across the investigated biorelevant conditions.

3.6.3 Visual Predictive Check (VPC)

Visual predictive checks were performed to evaluate the ability of the PBPK model to describe both the central tendency and variability of lurasidone pharmacokinetics. Observed concentration–time data digitized from the published pharmacokinetic profile reported by Loebel et al. (2013) [91] were compared with simulated population profiles generated using the validated PBPK model.

The simulated percentile ranges and corresponding observed plasma concentrations used for VPC analysis are summarized in Table S7, and VPC Curve is shown in Figure S6 as supplementary data.

The median simulated plasma concentrations ranged from 2.4 to 51.6 µmol/L, whereas the corresponding 5th and 95th percentile concentration ranges were 0.8–35.7 µmol/L and 6.3–72.4 µmol/L, respectively. Observed plasma concentrations ranged from 2.1 to 50.8 µmol/L over the study period. All observed plasma concentrations were contained within the simulated 5th–95th percentile prediction interval throughout the study period. The highest observed concentration (50.8 µmol/L) and median simulated concentration (51.6 µmol/L) were both observed at 2 h, demonstrating close agreement between observed and simulated pharmacokinetic profiles.

Overall, the prediction error analysis, fold error assessment, goodness-of-fit analysis, and visual predictive checks collectively demonstrated good agreement between simulated and observed pharmacokinetic behavior. These findings support the application of the developed PBPK model for PBPK-assisted IVISc analysis and sensitivity assessment of lurasidone hydrochloride.

3.7 PBPK Simulation in Hepatic Impairment Population

The validated PBPK model was applied to subjects with hepatic impairment to investigate the influence of altered hepatic function on lurasidone pharmacokinetics. The predicted pharmacokinetic parameters are presented in Table S8 as supplementary data and plasma time profiles mentioned in the figure VII

Figure VII. Simulated plasma concentration–time profiles of lurasidone in healthy adults and subjects with hepatic impairment.

Compared with healthy adults, the hepatic impairment population demonstrated increased systemic exposure. The predicted Cmax increased from 64.2 to 77.0 µmol/L, while AUCtend increased from 5138.05 to 5395.20 µmol·min/L. Tmax showed only a minor increase from 2.0 to 2.3 h.

The results indicate that hepatic impairment primarily affected the extent of drug exposure rather than the rate of absorption. The marked increase in AUCtend suggests reduced drug clearance in the hepatic impairment population.

4. Regulatory Relevance and Model-Informed Drug Development Perspective

The present study demonstrates the applicability of dissolution-informed physiologically based pharmacokinetic (PBPK) modeling within the framework of Model-Informed Drug Development (MIDD). Recent regulatory guidance issued by the United States Food and Drug Administration (FDA) and the International Council for Harmonisation (ICH) recognizes PBPK modeling as an important quantitative tool for supporting drug development and regulatory decision-making. PBPK models may be used for biopharmaceutics applications, food-effect assessment, special population predictions, formulation development, and risk assessment. [87, 88]

The FDA guidance entitled *The Use of Physiologically Based Pharmacokinetic Analyses—Biopharmaceutics Applications for Oral Drug Product Development, Manufacturing Changes, and Controls* highlights the role of PBPK modeling in establishing clinically relevant dissolution specifications and developing biopredictive dissolution methods for orally administered drug products.[87]

The integration of experimentally generated biorelevant dissolution data with PBPK simulations in the present study aligns with current regulatory initiatives promoting physiologically based biopharmaceutics modeling (PBBM). Such approaches may support food-effect evaluation, virtual bioequivalence assessment, formulation optimization, and reduced dependence on extensive clinical studies.[89]

Furthermore, the recent ICH M15 guidance on Model-Informed Drug Development emphasizes the importance of model development, verification, validation, and documentation for regulatory applications (ICH, 2025). The development, validation, sensitivity analysis, and external evaluation performed in the present study are consistent with these principles and demonstrate the potential regulatory utility of PBPK-assisted IVISc approaches. Similar regulatory applications of PBPK modeling have been highlighted by.[90]

Therefore, the developed dissolution-informed PBPK framework may provide a useful tool for formulation development, special population assessment, food-effect prediction, and model-informed pharmaceutical decision-making.

5. Discussion

The present study investigated whether integration of biorelevant dissolution testing with physiologically based pharmacokinetic (PBPK) modeling could establish a mechanistic in vitro–in silico correlation (IVISc) for lurasidone hydrochloride, a BCS Class II drug exhibiting dissolution-limited absorption and a pronounced positive food effect. The developed framework successfully translated dissolution behavior generated under physiologically relevant gastrointestinal conditions into predicted pharmacokinetic outcomes, thereby supporting the proposed hypothesis that dissolution profiles obtained under fasted and fed conditions can predict systemic drug exposure.

The validated UV–Visible spectrophotometric method demonstrated satisfactory accuracy, precision, and sensitivity for dissolution sample analysis. Calibration curves generated in each biorelevant medium minimized matrix effects and ensured reliable quantification. Dissolution studies performed in FaSSGF, FeSSGF, FaSSIF, and FeSSIF demonstrated that gastrointestinal physiological conditions significantly influenced the dissolution behavior of lurasidone hydrochloride. The highest drug release was observed in FeSSGF (85.1%), followed by FeSSIF (78.8%), FaSSGF (61.8%), and FaSSIF (57.7%). One-way ANOVA revealed statistically significant differences among the investigated media ($p < 0.05$), confirming the influence of media composition on drug release. The relatively narrow 95% confidence intervals indicated good experimental reproducibility and increased confidence in the subsequent PBPK simulations that relied upon these dissolution inputs. [53, 54, 55]

The enhanced dissolution observed under fed-state conditions can primarily be attributed to increased concentrations of bile salts and phospholipids, which promote micellar solubilization and increase the apparent solubility of lurasidone. Delayed gastric emptying under fed conditions may additionally prolong drug residence time and allow greater dissolution before intestinal transit. Since lurasidone possesses high permeability but limited aqueous solubility, dissolution represents the principal rate-limiting step governing oral absorption. Consequently, improved solubilization under fed-state conditions increases the amount of dissolved drug available for absorption and ultimately enhances systemic exposure.

Kinetic analysis further supported the complex dissolution behavior of lurasidone. Although the Korsmeyer–Peppas model was originally developed to describe drug release from polymeric matrices, it is also widely employed as an empirical model to characterize release mechanisms when dissolution is governed by multiple concurrent processes. Among the investigated models, the Korsmeyer–Peppas model demonstrated the highest goodness-of-fit for most dissolution media ($R^2 = 0.9924–0.9995$). The release exponent values ($n = 0.586–0.753$) indicated anomalous or non-Fickian transport behavior, suggesting that drug release was governed by multiple mechanisms, including diffusion, solubilization, and dissolution processes. Such behavior is commonly observed for poorly water-soluble compounds in biorelevant media where dissolution and solubilization occur simultaneously.

Similarity factor (f_2) analysis demonstrated substantial differences between fasted and fed gastric conditions. The low similarity observed between FaSSGF and FeSSGF ($f_2 = 32.47$) indicates that gastric physiological conditions exert a strong influence on dissolution behavior. In contrast, FaSSIF and FeSSIF demonstrated greater similarity ($f_2 = 66.92$), suggesting comparatively smaller differences under intestinal conditions. These findings indicate that gastric conditions may contribute more significantly to the food-dependent dissolution behavior of lurasidone.

One of the principal objectives of the study was to establish a mechanistic relationship between dissolution behavior and pharmacokinetic performance through PBPK modeling. The developed PBPK model successfully integrated experimentally generated dissolution profiles with literature-derived physicochemical and physiological parameters. The rank order of dissolution performance (FeSSGF >

FeSSIF > FaSSGF > FaSSIF) was preserved in the predicted pharmacokinetic outcomes, indicating that dissolution behavior directly influenced systemic exposure.

The highest predicted Cmax and AUC values were obtained for FeSSGF, whereas the lowest exposure was observed for FaSSIF. This agreement strongly suggests that dissolution is a major determinant of lurasidone absorption variability and supports the mechanistic basis of the developed PBPK framework.

Unlike empirical IVIVC approaches, dissolution-informed PBPK modeling integrates experimentally generated dissolution data with physiological processes governing absorption, metabolism, and systemic disposition. Consequently, medium-specific dissolution behavior obtained under fasted and fed conditions was translated into dynamic gastrointestinal drug concentrations and corresponding plasma concentration –time profiles.[91]

The mechanistic relationship linking dissolution behavior, gastrointestinal physiology, and predicted pharmacokinetic performance is illustrated in Figure S7 as supplementary data. Increased bile salt concentrations under fed-state conditions promote mixed micelle formation, increase apparent solubility, and enhance drug dissolution. The resulting increase in dissolved drug concentration generates larger concentration gradients across the intestinal epithelium and increases passive diffusion, ultimately producing higher systemic exposure.

These findings are consistent with previous studies demonstrating the utility of dissolution-informed PBPK and physiologically based biopharmaceutics modeling (PBBM) approaches. Heimbach et al. [92] reported successful prediction of food-mediated pharmacokinetic changes using mechanistic models, while Koppikara et al. [93] demonstrated improved prediction of in vivo performance through incorporation of dissolution data into biopharmaceutic models. Similarly, McAllister et al. [94] highlighted the regulatory value of integrating biopredictive dissolution testing with PBPK modeling.

From a clinical perspective, the approximately 1.5–1.7-fold increase in predicted systemic exposure under fed conditions is consistent with the clinically reported positive food effect associated with lurasidone and supports current dosing recommendations requiring administration with food. These findings emphasize the importance of gastrointestinal physiology in achieving adequate therapeutic exposure and minimizing pharmacokinetic variability.

Sensitivity analysis was performed using parameters selected based on their established biological relevance and their recognized influence on PBPK predictions of oral drug absorption and systemic exposure. Sensitivity analysis identified solubility, CYP3A4-mediated clearance, oral dose, and effective permeability as the most influential determinants of systemic exposure. Solubility demonstrated the highest positive influence, whereas CYP3A4 clearance exerted the greatest negative effect on both Cmax and AUC. These observations reinforce the dissolution-limited nature of lurasidone absorption and highlight the combined importance of absorption and metabolism in determining systemic exposure.

The selected parameter ranges were based on literature-derived pharmacokinetic data and physiological variability available within the PK-Sim database, ensuring physiologically meaningful assessment of model sensitivity. The identification of these influential parameters may support formulation optimization and biopharmaceutical risk assessment during drug development.

The PBPK-assisted IVISc established in the present study demonstrated a strong positive relationship between dissolution extent and predicted systemic exposure, yielding an R^2 value of 0.9545. Media exhibiting greater dissolution consistently produced higher predicted AUC values, indicating effective translation of dissolution behavior into pharmacokinetic outcomes. Unlike conventional IVIVC approaches requiring extensive clinical data, the developed IVISc provides a mechanistic relationship between in vitro dissolution and in silico pharmacokinetic predictions.

Although the correlation was established using only four biorelevant media conditions, the results demonstrate the potential utility of PBPK-assisted IVISc as a predictive tool for evaluating food effects and formulation performance. Future investigations involving additional formulations and broader dissolution characteristics may further improve the statistical robustness of the developed correlation.

Model validation demonstrated satisfactory predictive performance of the developed PBPK framework. Visual predictive checks, goodness-of-fit analysis, fold-error analysis, and prediction-error calculations all demonstrated good agreement between simulated and observed pharmacokinetic data. Fold-error values ranged from 1.0367 to 1.0398, while prediction errors remained below 4%.

The low prediction errors indicate excellent model performance; however, the availability of limited validation datasets may partially contribute to the close agreement observed between predicted and observed data. Nevertheless, model construction was primarily based on independently reported physicochemical and physiological parameters rather than empirical fitting of pharmacokinetic outcomes. Furthermore, external pharmacokinetic data not used during model development were employed for validation, reducing the likelihood of model overfitting.

The developed PBPK model was subsequently applied to a hepatic impairment population to evaluate the influence of altered physiological conditions on lurasidone pharmacokinetics. Simulations were performed using the hepatic impairment population available in PK-Sim® representing Child–Pugh B (moderate hepatic impairment), in which physiological changes associated with reduced hepatic function and drug clearance are incorporated. Compared with healthy adults, hepatic impairment resulted in increased systemic exposure, with Cmax increasing from 64.2 to 77.0 µmol/L and AUCtend increasing from 5138.05 to 5395.20 µmol·min/L, while only minor changes in Tmax were observed. Because lurasidone undergoes extensive CYP3A4-mediated hepatic metabolism, reduced hepatic function decreases metabolic clearance and consequently increases systemic exposure. Hepatic impairment was selected as the special population in the present study because hepatic metabolism represents the primary elimination pathway for lurasidone and is therefore expected to have a greater impact on its pharmacokinetics than populations primarily characterized by changes in renal function or demographic factors. Evaluation of additional special populations, including elderly subjects, patients

with renal impairment, and individuals with obesity, may further extend the applicability of the developed PBPK model and should be considered in future investigations.

Because lurasidone undergoes extensive CYP3A4-mediated hepatic metabolism, reduced hepatic function decreases metabolic clearance and increases systemic exposure. The substantial increase in AUC observed in the hepatic impairment population highlights the importance of hepatic metabolism in determining lurasidone pharmacokinetics and demonstrates the ability of the PBPK model to predict pharmacokinetic changes in special populations.These findings illustrate the potential application of the developed model for dose optimization, risk assessment, and special population evaluation within a model-informed drug development framework.

From a broader pharmaceutical perspective, the integration of biorelevant dissolution testing with PBPK modeling represents an important component of Model-Informed Drug Development (MIDD). The developed approach enables mechanistic prediction of oral drug performance, supports food-effect assessment, facilitates formulation optimization, and may reduce dependence on extensive in vivo studies.

Recent regulatory guidance issued by the FDA and ICH recognizes PBPK modeling as an important quantitative tool for drug development and regulatory decision-making.[92, 93] The integration of experimentally generated dissolution data with PBPK simulations aligns with current physiologically based biopharmaceutics modeling (PBBM) initiatives and may support food-effect assessment, virtual bioequivalence studies, and formulation optimization.[94] Furthermore, the systematic model development, validation, sensitivity analysis, and special population simulations performed in the present study are consistent with current MIDD principles and demonstrate the potential regulatory utility of PBPK-assisted IVISc approaches.

The present study demonstrated that biorelevant dissolution profiles can be successfully integrated with physiologically based pharmacokinetic (PBPK) modeling to predict the pharmacokinetic performance of lurasidone hydrochloride. The developed PBPK-assisted in vitro–in silico correlation (IVISc) established a mechanistic relationship between dissolution behavior and systemic exposure under fasted and fed conditions. Model validation, sensitivity analysis, and simulations in a hepatic impairment population supported the predictive performance and applicability of the developed framework. These findings demonstrate the potential utility of dissolution-informed PBPK modeling for evaluating food effects, formulation performance, and pharmacokinetic behavior of poorly water-soluble drugs.

6. Study Limitations and Future Perspectives

The present study successfully established a dissolution-informed PBPK framework for lurasidone hydrochloride by integrating biorelevant dissolution data with mechanistic pharmacokinetic modeling. However, certain limitations should be acknowledged. The developed model was validated using literature-reported pharmacokinetic data and a single immediate-release formulation; therefore, external

validation using independent marketed formulations remains necessary to further establish model robustness and predictive performance.

Although biorelevant dissolution media provided physiologically relevant insights, they may not fully reproduce the complexity of the in vivo gastrointestinal environment. In addition, supersaturation and precipitation phenomena were represented mechanistically within the PBPK framework, while experimental precipitation kinetics were not evaluated. Physiological variability was incorporated through virtual population simulations; however, all sources of inter-individual variability may not have been fully captured.

Future investigations should focus on external validation using reference and generic lurasidone formulations by incorporating formulation-specific dissolution profiles into the developed PBPK model. Such studies may support formulation assessment, virtual bioequivalence evaluation, and broader regulatory applications. Furthermore, incorporation of precipitation kinetics, advanced physiological variability, and additional BCS Class II compounds may further improve the predictive capability and generalizability of the developed PBPK-assisted IVISc framework.

Declarations

Credit Author Contribution Statement

Sonal Y. Mhaske: Conceptualization, Literature review, Methodology, Investigation, Biorelevant dissolution experiments, PBPK model development and simulations, Data curation, Formal analysis, Visualization, Preparation of figures and tables, Writing – original draft, Writing – review & editing.

Dr. Minal R. Narkhede: Conceptualization, Supervision, Methodology, Scientific guidance, Interpretation of results, Project administration, Writing – review & editing, Final approval of the manuscript.

Dr. Jitendra Nehete: Data curation, Statistical methodology, Formal analysis, Validation, Statistical analysis and interpretation, Writing – review & editing.

Declaration of Competing Interest

The authors declare that they have no known competing financial interests or personal relationships that could have appeared to influence the work reported in this paper.

Funding Statement

This research did not receive any specific grant from funding agencies in the public, commercial, or not-for-profit sectors.

Data Availability Statement

The data supporting the findings of this study are available from the corresponding author upon reasonable request.

Acknowledgements

The authors thank the Department of Pharmaceutics, SMBT College of Pharmacy, Nashik, India, for providing laboratory facilities and technical support to carry out this research work.

References

1. Song T, Wang W, Wu Y, Liu C, Yuan L, Sun Z, Zhang J, Sun Y. Functional Liposomes Improve the Oral Absorption of Lurasidone Hydrochloride by Overcoming Multiple Absorption Barriers and Eliminating Food Effect. Int J Nanomed. 2025;20:4883–901. https://doi.org/10.2147/ijn.s512876.
2. Heng W, Su M, Cheng H, Shen P, Liang S, Zhang L, Wei Y, Gao Y, Zhang J, Qian S. Incorporation of complexation into coamorphous system dramatically enhances dissolution and eliminates gelation of amorphous lurasidone hydrochloride. Mol Pharm. 2019. https://doi.org/10.1021/acs.molpharmaceut.9b00772.
3. Kaur N, Narang A, Bansal A. Use of biorelevant dissolution and PBPK modeling to predict oral drug absorption. Eur J Pharm Biopharm. 2018;129:222–46. https://doi.org/10.1016/j.ejpb.2018.05.024.
4. Cheng L, Wong H. (2020). Food Effects on Oral Drug Absorption: Application of Physiologically Based Pharmacokinetic Modeling as a Predictive Tool. *Pharmaceutics, 12*. https://doi.org/10.3390/pharmaceutics12070672
5. Gao P, Shi Y, Miller JM. (2017). Development and Application of in vitro Two-Phase Dissolution Method for Poorly Water-Soluble Drugs. 233–58. https://doi.org/10.1201/9781315364537-12
6. Takano R, Sugano K, Higashida A, Hayashi Y, Machida M, Aso Y, Yamashita S. Oral Absorption of Poorly Water-Soluble Drugs: Computer Simulation of Fraction Absorbed in Humans from a Miniscale Dissolution Test. Pharm Res. 2006;23:1144–56. https://doi.org/10.1007/s11095-006-0162-4.
7. Charalabidis A, Sfouni M, Bergström CAS, Macheras P. The Biopharmaceutics Classification System (BCS) and the Biopharmaceutics Drug Disposition Classification System (BDDCS): Beyond guidelines. Int J Pharm. 2019;566:264–81. https://doi.org/10.1016/j.ijpharm.2019.05.041.
8. Miura I, Horikoshi S, Ichinose M, Suzuki Y, Watanabe K. Lurasidone for the Treatment of Schizophrenia: Design, Development, and Place in Therapy. Drug Des Devel Ther. 2023;17:3023–31. https://doi.org/10.2147/dddt.s366769.
9. Ekinci R, Uygun E. Mechanism of Action and Uses of Lurasidone, A New Generation of Antipsychotics: A Review. Psychiatry Behav Sci. 2025. https://doi.org/10.5455/pbs.20241104052122.
10. Okubo R, Hasegawa T, Fukuyama K, Shiroyama T, Okada M. (2021). Current Limitations and Candidate Potential of 5-HT7 Receptor Antagonism in Psychiatric Pharmacotherapy. *Frontiers in Psychiatry, 12*. https://doi.org/10.3389/fpsyt.2021.623684

11. Tarzian M, Soudan M, Alhajji M, Ndrio M, Fakoya A. Lurasidone for Treating Schizophrenia and Bipolar Depression: A Review of Its Efficacy. Cureus. 2023;15. https://doi.org/10.7759/cureus.38071.
12. Greenberg W, Citrome L. Pharmacokinetics and Pharmacodynamics of Lurasidone Hydrochloride, a Second-Generation Antipsychotic: A Systematic Review of the Published Literature. Clin Pharmacokinet. 2017;56:493–503. https://doi.org/10.1007/s40262-016-0465-5.
13. Siwek M, Krupa A, Wąsik A. Lurasidone – pharmacodynamic and pharmacokinetic properties, clinical potential and interaction risk. Pharmacotherapy Psychiatry Neurol. 2020. https://doi.org/10.33450/10.33450/fpn.2020.06.002.
14. Gangane P, Ingle P, Rabade V, Sawarkar H. Formulation and Characterization of Chitosan Based Oral Nanoparticles of Poorly Water-Soluble Drug Lurasidone Hydrochloride. Indian J Pharm Educ Res. 2025. https://doi.org/10.5530/ijper.20253872.
15. Deepika D, Kumar V. The Role of Physiologically Based Pharmacokinetic Model (PBPK) New Approach Methodology (NAM) in Pharmaceuticals and Environmental Chemical Risk Assessment. Int J Environ Res Public Health. 2023;20. https://doi.org/10.3390/ijerph20043473.
16. Ozbek O, Genc DE, Ulgen KO. Advances in Physiologically Based Pharmacokinetic (PBPK) Modeling of Nanomaterials. ACS Pharmacol Translational Sci. 2024;7:2251–79. https://doi.org/10.1021/acsptsci.4c00250.
17. Lin L, Wong H. (2017). Predicting Oral Drug Absorption: Mini Review on Physiologically-Based Pharmacokinetic Models. *Pharmaceutics, 9*. https://doi.org/10.3390/pharmaceutics9040041
18. A SV, Nayak U, Sathyanarayana MB, Chaudhari BB, Bhat K. Formulation Strategy of BCS-II Drugs by Coupling Mechanistic In-Vitro and Nonclinical In-Vivo Data with PBPK: Fundamentals of Absorption-Dissolution to Parameterization of Modelling and Simulation. AAPS PharmSciTech. 2025;26. https://doi.org/10.1208/s12249-025-03093-9.
19. Chou P, Shannar A, Pan Y, Dave P, Xu J, Kong A-N. Application of Physiologically Based Pharmacokinetic (PBPK) Model in Drug Development and in Dietary Phytochemicals. Curr Pharmacol Rep. 2025;11. https://doi.org/10.1007/s40495-025-00427-w.
20. Foti RS. (2024). Utility of PBPK Modeling in Predicting and Characterizing Clinical Drug Interactions. *Drug metabolism and disposition: the biological fate of chemicals*. https://doi.org/10.1124/dmd.123.001384
21. Sun Z, Zhao N, Zhao X, Wang Z, Liu Z, Cui Y. Food Drug Adm European J Pharm sciences: official J Eur Federation Pharm Sciences. 2024;106838. https://doi.org/10.1016/j.ejps.2024.106838. Application of Physiologically Based Pharmacokinetic Modeling of Novel Drugs Approved by the U.S.
22. Rowland M, Lesko LJ, Rostami-Hodjegan A. Physiologically Based Pharmacokinetics Is Impacting Drug Development and Regulatory Decision Making. CPT: Pharmacometrics Syst Pharmacol. 2015;4:313–5. https://doi.org/10.1002/psp4.52.

23. Paul P, Colin P, Tshinanu FM, Versantvoort C, Manolis E, Blake K. Current Use of Physiologically Based Pharmacokinetic modeling in New Medicinal Product Approvals at EMA. Clin Pharmacol Ther. 2025;117:808–17. https://doi.org/10.1002/cpt.3525.
24. Jamei M, Abrahamsson B, Brown J, Bevernage J, Bolger M, Heimbach T, Karlsson EM, Kotzagiorgis E, Lindahl A, McAllister M, Mullin J, Pepin X, Tistaert C, Turner D, Kesisoglou F. (2020). Current status and future opportunities for incorporation of dissolution data in pbpk modeling for pharmaceutical development and regulatory applications: orbito consortium commentary. *European journal of pharmaceutics and biopharmaceutics: official journal of Arbeitsgemeinschaft fur Pharmazeutische Verfahrenstechnik e.V*. https://doi.org/10.1016/j.ejpb.2020.08.005
25. Otsuka K, Shono Y, Dressman J. Coupling biorelevant dissolution methods with physiologically based pharmacokinetic modelling to forecast in-vivo performance of solid oral dosage forms. J Pharm Pharmacol. 2013;65. https://doi.org/10.1111/jphp.12059.
26. Golhar A, Pillai M, Dhakne P, Rajput N, Jadav T, Sengupta P. Progressive tools and critical strategies for development of best fit PBPK model aiming better in vitro-in vivo correlation. Int J Pharm. 2023;123267. https://doi.org/10.1016/j.ijpharm.2023.123267.
27. Shono Y, Jantratid E, Janssen N, Kesisoglou F, Mao Y, Vertzoni M, Reppas C, Dressman J. Prediction of food effects on the absorption of celecoxib based on biorelevant dissolution testing coupled with physiologically based pharmacokinetic modeling. Eur J Pharm biopharmaceutics: official J Arbeitsgemeinschaft fur Pharmazeutische Verfahrenstechnik e V. 2009;73(1):107–14. https://doi.org/10.1016/j.ejpb.2009.05.009.
28. Kushwah V, Arora S, Katona MT, Modhave D, Fröhlich E, Paudel A. On Absorption Modeling and Food Effect Prediction of Rivaroxaban, a BCS II Drug Orally Administered as an Immediate-Release Tablet. Pharmaceutics. 2021;13. https://doi.org/10.3390/pharmaceutics13020283.
29. Wang J, Huang B, Dai J, Chen G, Ren L. Inclusion complex of lurasidone hydrochloride with Sulfobutylether-β-cyclodextrin has enhanced oral bioavailability and no food effect. Am J translational Res. 2022;14 3:1495–506.
30. Lex T, Rodriguez JD, Zhang L, Jiang W, Gao Z. Development of In Vitro Dissolution Testing Methods to Simulate Fed Conditions for Immediate Release Solid Oral Dosage Forms. AAPS J. 2022;24. https://doi.org/10.1208/s12248-022-00690-5.
31. Jantratid E, Janssen N, Reppas C, Dressman J. Dissolution Media Simulating Conditions in the Proximal Human Gastrointestinal Tract: An Update. Pharm Res. 2008;25:1663–76. https://doi.org/10.1007/s11095-008-9569-4.
32. Leigh M, Kloefer B, Schaich M. Comparison of the Solubility and Dissolution of Drugs in FastedState Biorelevant Media (FaSSIF and FaSSIF-V2). Dissolution Technol. 2013;20:44–50. https://doi.org/10.14227/dt200313p44.
33. Mudie DM, Samiei N, Marshall D, Amidon G, Bergström CAS. Selection of In Vivo Predictive Dissolution Media Using Drug Substance and Physiological Properties. AAPS J. 2020;22. https://doi.org/10.1208/s12248-020-0417-8.

34. Phillips DJ, Pygall S, Cooper V, Mann J. Overcoming sink limitations in dissolution testing: a review of traditional methods and the potential utility of biphasic systems. J Pharm Pharmacol. 2012;64. https://doi.org/10.1111/j.2042-7158.2012.01523.x.
35. Hate SS, Thompson SA, Singaraju AB. Impact of sink conditions on drug release behavior of controlled-release formulations. J Pharm Sci. 2024. https://doi.org/10.1016/j.xphs.2024.10.032.
36. Patel P, Parmar R. Validation of UV spectrophotometric method for estimation of bedaquiline fumarate in bulk and pharmaceutical formulations. J Res Pharm. 2024. https://doi.org/10.29228/jrp.786.
37. Jamil RG, Polli J. Prediction of In Vitro Drug Dissolution into Fed-state Biorelevant Media: Contributions of Solubility Enhancement and Relatively Low Colloid Diffusivity. Eur J Pharm sciences: official J Eur Federation Pharm Sci. 2022;106179. https://doi.org/10.1016/j.ejps.2022.106179.
38. Jamil RG, Polli J. Prediction of In Vitro Drug Dissolution into Fasted-state Biorelevant Media: Contributions of Solubility Enhancement and Relatively Low Colloid Diffusivity. Eur J Pharm sciences: official J Eur Federation Pharm Sci. 2022;106210. https://doi.org/10.1016/j.ejps.2022.106210.
39. International Council for Harmonisation. Validation of analytical procedures: text and methodology Q2(R1) [Internet]. Geneva: ICH; 2005. Nov [cited 2026 Jun 10]ICH Q2(R1) Guideline.
40. More B, Wakte P, Bhusari S. Validated UV-Visible Spectrophotometric Method for Quantitative Analysis of Glycyrrhizin. J Drug Delivery Ther. 2026. https://doi.org/10.22270/jddt.v16i1.7523.
41. Benazir SB, Archana J, Sumakanth M. Method Development and Validation of Empagliflozin in Bulk and Pharmaceutical Dosage Form using UV Spectroscopy. Asian J Pharm Anal. 2021;11:123–6. https://doi.org/10.52711/2231-5675.2021.00021.
42. Cascone S. Modeling and comparison of release profiles: Effect of the dissolution method. Eur J Pharm Sci. 2017;106:352–61. https://doi.org/10.1016/j.ejps.2017.06.021.
43. Jamil RG, Xu T, Shah HS, Adhikari A, Sardhara R, Nahar K, Morris K, Polli J. Similarity of dissolution profiles from biorelevant media: Assessment of interday repeatability, interanalyst repeatability, and interlaboratory reproducibility using ibuprofen and ketoconazole tablets. Eur J Pharm sciences: official J Eur Federation Pharm Sci. 2020;156:105573. https://doi.org/10.1016/j.ejps.2020.105573.
44. Romodanovsky DP, Goryachev D. (2021). Alternative Methods for Dissolution Profile Comparison in the Dissolution Test. *Drug development & registration*. https://doi.org/10.33380/2305-2066-2021-10-4-197-207
45. Muselík J, Komersová A, Kubová K, Matzick K, Skalická B. A Critical Overview of FDA and EMA Statistical Methods to Compare In Vitro Drug Dissolution Profiles of Pharmaceutical Products. Pharmaceutics. 2021;13. https://doi.org/10.3390/pharmaceutics13101703.
46. Costa P. (2001). An alternative method to the evaluation of similarity factor in dissolution testing. *International journal of pharmaceutics, 220 1–2*, 77–83. https://doi.org/10.1016/s0378-5173(01)00651-2

47. Stevens RE, Gray V, Dorantes A, Gold LC, Pham L. Scientific and Regulatory Standards for Assessing Product Performance Using the Similarity Factor, f2. AAPS J. 2015;17:301–6. https://doi.org/10.1208/s12248-015-9723-y.
48. Hsu J, Hsu M, Liao C, Hsu H. On the characteristics of the FDA's similarity factor for comparison of drug dissolution. J Food Drug Anal. 2020;6:553–8. https://doi.org/10.38212/2224-6614.2899.
49. Boddu R, Parsa K, Pandya P, Kollipara S. Dissolution Profiles Comparison Using Various Model Independent Statistical Approaches: Can We Increase Chance of Similarity? Pharm Res. 2025;42:1347–62. https://doi.org/10.1007/s11095-025-03892-6.
50. Bermejo M, Hens B, Dickens JR, Mudie DM, Paixão P, Tsume Y, Shedden K, Amidon G, Pharmaceutics. 12. https://doi.org/10.3390/pharmaceutics12010074
51. Nagabandi V, Kumar MS, Prasad G, Someshwar K, Varaprasad A. Comparative Dissolution Studies of Marketed Preparations and Treatment of Data by Using ANOVA. Int J Adv Pharm Sci. 2010;1. https://doi.org/10.5138/161.
52. Hespanhol L, Vallio CS, Costa LM, Saragiotto B. Understanding and interpreting confidence and credible intervals around effect estimates. Braz J Phys Ther. 2019. https://doi.org/10.1016/j.bjpt.2018.12.006.
53. Lew MJ. Good statistical practice in pharmacology Problem 2. Br J Pharmacol. 2007;152. https://doi.org/10.1038/sj.bjp.0707372.
54. Kesisoglou F, Xia B, Agrawal N. Comparison of Deconvolution-Based and Absorption Modeling IVIVC for Extended-Release Formulations of a BCS III Drug Development Candidate. AAPS J. 2015;17:1492–500. https://doi.org/10.1208/s12248-015-9816-7.
55. Soni T, Chotai N. Assessment of Dissolution Profile of Marketed Aceclofenac Formulations. J Young Pharmacists: JYP. 2010;2:21–6. https://doi.org/10.4103/0975-1483.62208.
56. Cuquerella-Gilabert M, Reig-López J, Serna J, Rueda-Ferreiro A, Merino-Sanjuán M, Mangas-Sanjuán V, Sánchez-Herrero S. Phys-DAT: A physiologically based pharmacokinetic model for unraveling the dissolution, transit and absorption processes using PhysPK®. Comput Methods Programs Biomed. 2023;243:107929. https://doi.org/10.1016/j.cmpb.2023.107929.
57. D'Ambrosio A, Itaj F, Cacace F, Piemonte V. Mathematical Modeling of the Gastrointestinal System for Preliminary Drug Absorption Assessment. Bioengineering. 2024;11. https://doi.org/10.3390/bioengineering11080813.
58. Ezuruike U, Zhang M, Pansari A, De Sousa Mendes M, Pan X, Neuhoff S, Gardner I. Guide to development of compound files for PBPK modeling in the Simcyp population-based simulator. CPT: Pharmacometrics Syst Pharmacol. 2022;11:805–21. https://doi.org/10.1002/psp4.12791.
59. Dahlgren D, Lennernäs H. Intestinal Permeability and Drug Absorption: Predictive Experimental, Computational and In Vivo Approaches. Pharmaceutics. 2019;11. https://doi.org/10.3390/pharmaceutics11080411.
60. Ahmad A, Pepin X, Aarons L, Wang Y, Darwich A, Wood MJ, Tannergren C, Karlsson EM, Patterson C, Thörn H, Ruston L, Mattinson A, Carlert S, Berg S, Murphy D, Engman H, Laru J, Barker R, Flanagan T,

Rostami-Hodjegan A. (2020). IMI - Oral biopharmaceutics tools project - Evaluation of bottom-up PBPK prediction success part 4: Prediction accuracy and software comparisons with improved data and modelling strategies. *European journal of pharmaceutics and biopharmaceutics: official journal of Arbeitsgemeinschaft fur Pharmazeutische Verfahrenstechnik e.V*. https://doi.org/10.1016/j.ejpb.2020.08.006

61. Kostewicz E, Aarons L, Bergstrand M, Bolger M, Galetin A, Hatley O, Jamei M, Lloyd RS, Pepin X, Rostami-Hodjegan A, Sjögren E, Tannergren C, Turner D, Wagner C, Weitschies W, Dressman J. PBPK models for the prediction of in vivo performance of oral dosage forms. Eur J Pharm sciences: official J Eur Federation Pharm Sci. 2014;57:300–21. https://doi.org/10.1016/j.ejps.2013.09.008.
62. Ishibashi T, Horisawa T, Tokuda K, Ishiyama T, Ogasa M, Tagashira R, Matsumoto K, Nishikawa H, Ueda Y, Toma S, Ohnuma T. Pharmacological profile of lurasidone, a novel antipsychotic agent with potent 5-HT7 and 5-HT1A receptor activity. J Pharmacol Exp Ther. 2010;334(1):171–81. https://doi.org/10.1124/jpet.110.167346.
63. Wishart, D. S., Feunang, Y. D., Guo, A. C., Lo, E. J., Marcu, A., Grant, J. R., Sajed,T., Johnson, D., Li, C., Sayeeda, Z., Assempour, N., Iynkkaran, I., Liu, Y., Maciejewski,A., Gale, N., Wilson, A., Chin, L., Cummings, R., Le, D., … Wilson, M. (2018). DrugBank 5.0: A major update to the DrugBank database for 2018. Nucleic Acids Research, 46(D1), D1074–D1082. https://doi.org/10.1093/nar/gkx1037.
64. Kim S, Chen J, Cheng T, Gindulyte A, He J, He S, Li Q, Shoemaker BA, Thiessen PA, Yu B, Zaslavsky L, Zhang J, Bolton EE. PubChem 2023 update. Nucleic Acids Res. 2023;51(D1):D1373–80. https://doi.org/10.1093/nar/gkac956.
65. Sunovion Pharmaceuticals Inc. Latuda® (lurasidone hydrochloride) tablets prescribing information. Sunovion Pharmaceuticals Inc; 2023. https://www.latuda.com.
66. Curry L, Alrubia S, Bois FY, Clayton R, El-Khateeb E, Johnson TN, Faisal M, Neuhoff S, Wragg K, Rostami-Hodjegan A. A guide to developing population files for physiologically based pharmacokinetic modeling in the Simcyp Simulator. CPT: Pharmacometrics Syst Pharmacol. 2024;13:1429–47. https://doi.org/10.1002/psp4.13202.
67. Hörter D, Dressman J. (1997). Influence of physicochemical properties on dissolution of drugs in the gastrointestinal tract. *Advanced drug delivery reviews, 46 1–3*, 75–87. https://doi.org/10.1016/s0169-409x(00)00130-7
68. Frechen S, Rostami-Hodjegan A. Quality Assurance of PBPK Modeling Platforms and Guidance on Building, Evaluating, Verifying and Applying PBPK Models Prudently under the Umbrella of Qualification: Why, When, What, How and By Whom? Pharm Res. 2022;39:1733–48. https://doi.org/10.1007/s11095-022-03250-w.
69. Shebley M, Sandhu P, Riedmaier AE, Jamei M, Narayanan R, Patel A, Peters S, Reddy V, Zheng M, De Zwart L, Bénéton M, Bouzom F, Chen J, Chen Y, Cleary Y, Collins C, Dickinson G, Djebli N, Einolf H, Rowland M. Physiologically Based Pharmacokinetic Model Qualification and Reporting Procedures for Regulatory Submissions: A Consortium Perspective. Clin Pharmacol Ther. 2018;104:88–110. https://doi.org/10.1002/cpt.1013.

70. McNally K, Cotton R, Loizou G. (2011). A Workflow for Global Sensitivity Analysis of PBPK Models. *Frontiers in Pharmacology, 2*. https://doi.org/10.3389/fphar.2011.00031
71. Le A-D, Wearing H, Li D. Streamlining physiologically based pharmacokinetic model design for intravenous delivery of nanoparticle drugs. CPT: Pharmacometrics Syst Pharmacol. 2022;11:409–24. https://doi.org/10.1002/psp4.12762.
72. Domínguez-Romero E, Mazurenko S, Scheringer M, Santos VMDAP, Evelo C, Anton M, Hancock JM, Županič A, Suárez-Diez M. Making PBPK models more reproducible in practice. Brief Bioinform. 2024;25. https://doi.org/10.1093/bib/bbae569.
73. Cheng Y-H, Thomas S, Tsang YC, Almeida S, Ashraf M, Fotaki N, Heimbach T, Patel N, Shah H, Jiang X, Kim M-J, Moody R, Rostami-Hodjegan A, Singh R, Zhao L, Babiskin A, Wu F. Advances in Physiologically Based Pharmacokinetic (PBPK) Modeling and its Regulatory Utility to Support Oral Drug Product Development and Harmonization. Pharm Res. 2025;42:819–33. https://doi.org/10.1007/s11095-025-03849-9.
74. Yuvaneshwari K, Kollipara S, Ahmed T, Chachad S. Applications of PBPK/PBBM modeling in generic product development: An industry perspective. J Drug Deliv Sci Technol. 2022. https://doi.org/10.1016/j.jddst.2022.103152.
75. Kushwah V, Arora S, Katona MT, Modhave D, Fröhlich E, Paudel A. On Absorption Modeling and Food Effect Prediction of Rivaroxaban, a BCS II Drug Orally Administered as an Immediate-Release Tablet. Pharmaceutics. 2021;13. https://doi.org/10.3390/pharmaceutics13020283.
76. Clewell H, Lee TS, Carpenter RL. Sensitivity of physiologically based pharmacokinetic models to variation in model parameters: methylene chloride. Risk analysis: official publication Soc Risk Anal. 1994;14(4):521–31. https://doi.org/10.1111/j.1539-6924.1994.tb00268.x.
77. Najjar A, Hamadeh A, Krause S, Schepky A, Edginton AN. Global sensitivity analysis of Open Systems Pharmacology Suite physiologically based pharmacokinetic models. CPT: Pharmacometrics Syst Pharmacol. 2024;13:2052–67. https://doi.org/10.1002/psp4.13256.
78. Liu D, Li L, Rostami-Hodjegan A, Bois F, Jamei M. Considerations and Caveats when Applying Global Sensitivity Analysis Methods to Physiologically Based Pharmacokinetic Models. AAPS J. 2020;22. https://doi.org/10.1208/s12248-020-00480-x.
79. Tang C, Ouyang C, Chen W, Zou C, Huang J, Cui C, Yang S, Guo C, Yang X-Y, Lin Y, Pei Q, Yang G-P. (2021). Prediction of pharmacokinetic parameters of inhaled indacaterol formulation in healthy volunteers using physiologically based pharmacokinetic (PBPK) model. *European journal of pharmaceutical sciences: official journal of the European Federation for Pharmaceutical Sciences*, 106055. https://doi.org/10.1016/j.ejps.2021.106055
80. Heimbach T, Chen Y, Chen J, Dixit V, Parrott N, Peters S, Poggesi I, Sharma P, Snoeys J, Shebley M, Tai G, Tse S, Upreti V, Wang Y-H, Tsai A, Xia B, Zheng M, Zhu AZX, Hall S. Physiologically Based Pharmacokinetic Modeling in Renal and Hepatic Impairment Populations: A Pharmaceutical Industry Perspective. Clin Pharmacol Ther. 2020;110:297–310. https://doi.org/10.1002/cpt.2125.

81. Bai C-Y, Zhang J, Xu X, Li X, Zhang T. Establishing virtual bioequivalence and bio-related dissolution specifications for naproxen using physiologically based pharmacokinetic modeling and in vitro biorelevant dissolution testing. Drug Dev Ind Pharm. 2025;51:895–906. https://doi.org/10.1080/03639045.2025.2515999.
82. Rodríguez-Fernández K, Gómez-Mantilla J, Shukla S, Stopfer P, Sieger P, Mangas-Sanjuán V, Peters S. Evaluation of Solubility-Limited Absorption as a Surrogate to Predicting Positive Food Effect of BCS II/IV Drugs. Clin Pharmacokinet. 2025;64:373–85. https://doi.org/10.1007/s40262-025-01473-9.
83. Van Borselen MV, Sluijterman L, Greupink R, De Wildt SD. Towards More Robust Evaluation of the Predictive Performance of Physiologically Based Pharmacokinetic Models: Using Confidence Intervals to Support Use of Model-Informed Dosing in Clinical Care. Clin Pharmacokinet. 2024;63:343–55. https://doi.org/10.1007/s40262-023-01326-3.
84. Pasha M, Zamir A, Rasool M, Saeed H, Ahmad T, Alqahtani NS, Alqahtani L, Alqahtani F. A Comprehensive Physiologically Based Pharmacokinetic Model for Predicting Vildagliptin Pharmacokinetics: Insights into Dosing in Renal Impairment. Pharmaceuticals. 2024;17. https://doi.org/10.3390/ph17070924.
85. Silva LL, Silvola RM, Haas D, Quinney S. Physiologically based pharmacokinetic modelling in pregnancy: Model reproducibility and external validation. Br J Clin Pharmacol. 2021;88:1441–51. https://doi.org/10.1111/bcp.15018.
86. Loebel A, Cucchiaro J, Silva R, Kroger H, Sarma K, Xu J et al. Lurasidone monotherapy in the treatment of schizophrenia: pharmacokinetic and clinical evaluation. *Clin Drug Investig.* 2013;33(9):675–685. Available from: https://doi.org/10.1007/s40261-013-0114-z
87. Food US, Drug Administration. The use of physiologically based pharmacokinetic analyses—Biopharmaceutics applications for oral drug product development, manufacturing changes, and controls: Guidance for industry. U.S. Food and Drug Administration; 2020. https://www.fda.gov/media/149580/download.
88. International Council for Harmonisation. (2025). M15 guideline: General principles for model-informed drug development. Int Council Harmonisation. https://www.ich.org/page/multidisciplinary-guidelines
89. Mackie CE, Stamatopoulos K, Vertzoni M, Augustijns P, Reppas C, Dressman J. Physiologically based biopharmaceutics modeling: Current status and future opportunities. Eur J Pharm Sci. 2024;196:106746. https://doi.org/10.1016/j.ejps.2024.106746.
90. Wu F, Zhao P, Zhang L, Lesko LJ. Regulatory utility of physiologically based pharmacokinetic modeling in drug development and evaluation. Clin Pharmacol Ther. 2023;113(3):535–48. https://doi.org/10.1002/cpt.2806.
91. Stillhart C, Pepin X, Tistaert C, Good D, Bergh A, Parrott N, Kesisoglou F. PBPK Absorption Modeling: Establishing the In Vitro–In Vivo Link—Industry Perspective. AAPS J. 2019;21. https://doi.org/10.1208/s12248-019-0292-3.

92. Heimbach T, Xia B, Lin TH, He H. Physiologically based pharmacokinetic modeling for food-effect prediction: Current practices, gaps, and future directions. Mol Pharm. 2021;18(4):1267–85. https://doi.org/10.1021/acs.molpharmaceut.0c01087.
93. Kollipara S, Vysyaraju K, Kesisoglou F, Vertzoni M, Reppas C. Role of physiologically based biopharmaceutics modeling (PBBM) in supporting fed bioequivalence study waivers: Regulatory outlook, case studies, and future perspectives. J Pharm Sci. 2024;113(2):523–37. https://doi.org/10.1016/j.xphs.2023.10.021.
94. McAllister, M., Flanagan, T., Cole, S., Abend, A., Kotzagiorgis, E., Limberg, J.,Mead, H., Mangas-Sanjuan, V., Dickinson, P. A., Moir, A., Pepin, X., Zhou, D., Tistaert,C., Dokoumetzidis, A., Anand, O., Le Merdy, M., Turner, D. B., Griffin, B. T., Darwich,A., … Mackie, C. (2022). Developing clinically relevant dissolution specifications(CRDSs) for oral drug products: Virtual webinar series. Pharmaceutics, 14(5), 1010. https://doi.org/10.3390/pharmaceutics14051010.

Figures

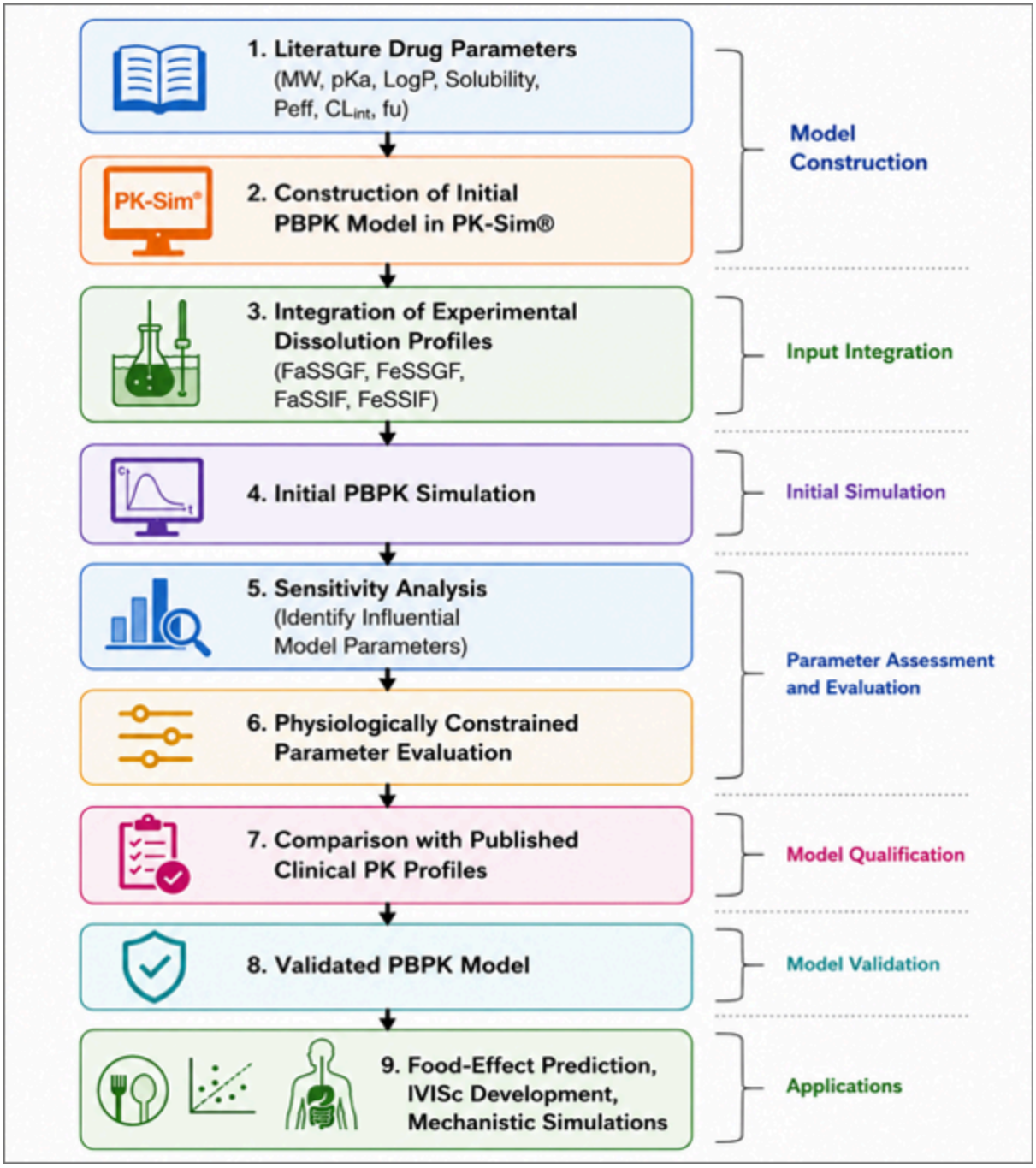


Figure 1

Workflow of PBPK model development and parameter optimization.

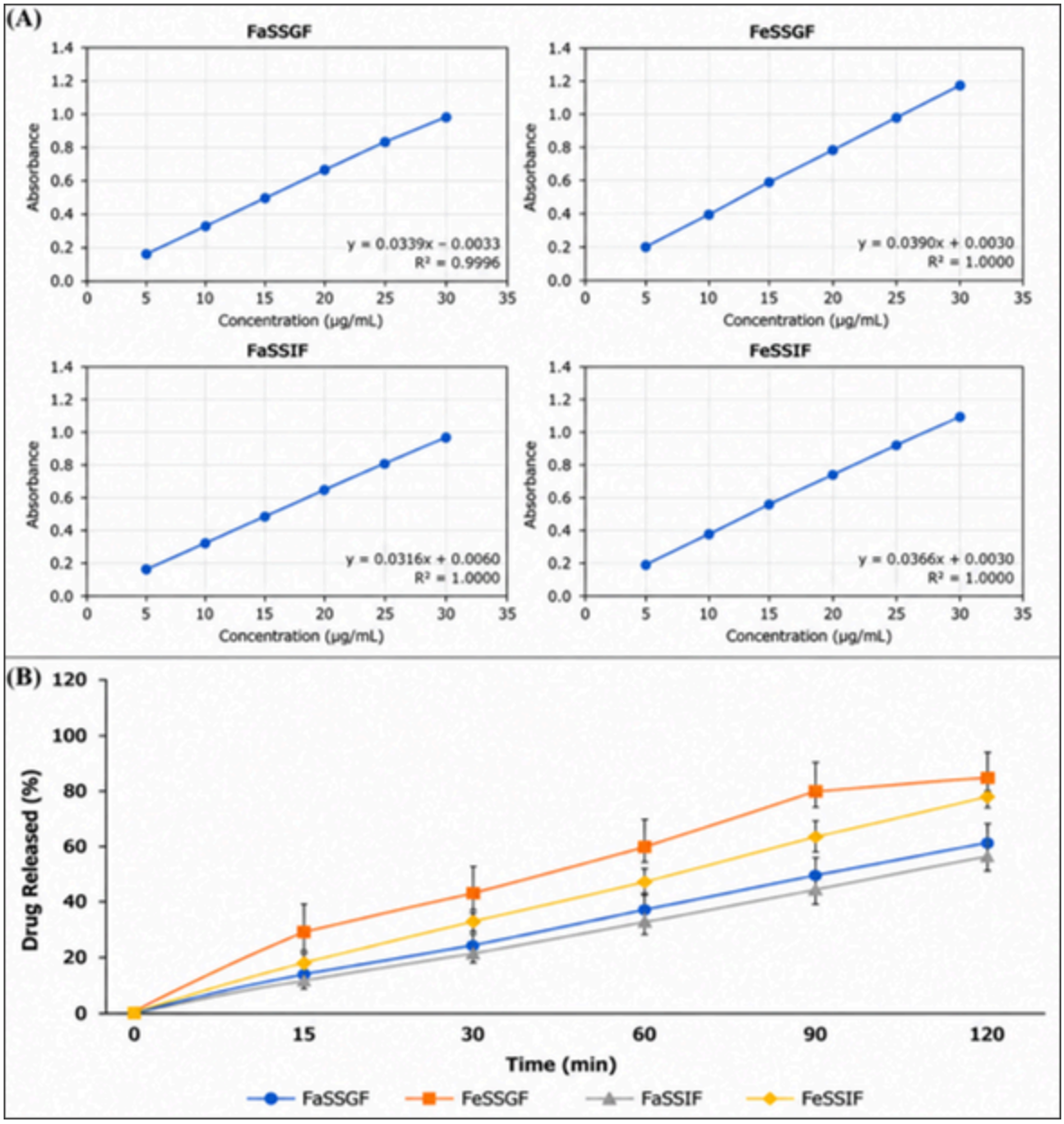


Figure 2

Analytical calibration curves and dissolution profiles of lurasidone hydrochloride in biorelevant media. (A) Calibration curves obtained in FaSSGF, FeSSGF, FaSSIF, and FeSSIF demonstrating excellent linearity across the concentration range of 5–30 µg/mL ($R^2 \geq 0.999$). (B) Comparative dissolution profiles of lurasidone hydrochloride in fasted- and fed-state simulated gastric and intestinal media over 120 min (mean ± SD, n = 3).

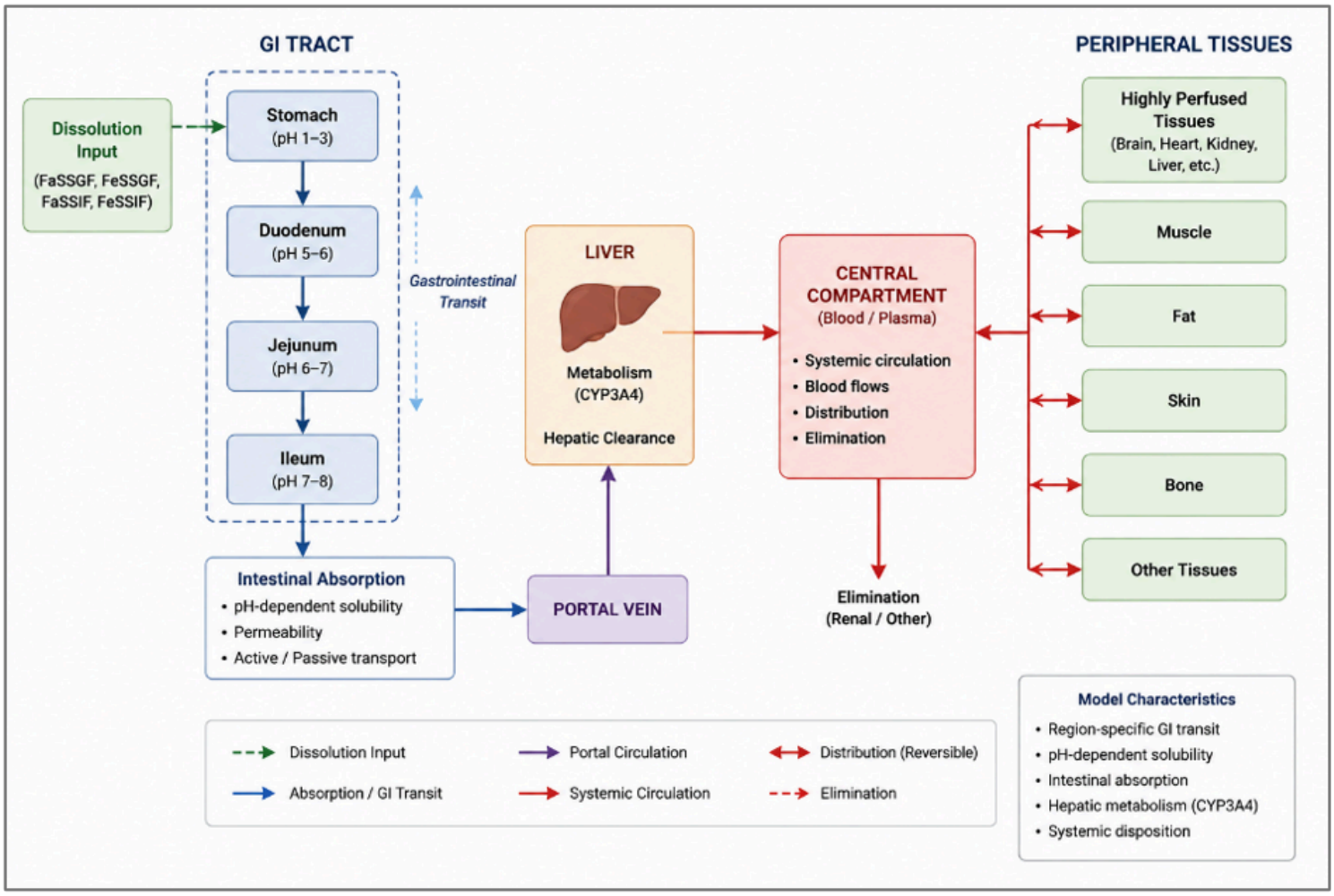


Figure 3

Schematic representation of the PBPK model architecture developed for lurasidone hydrochloride in PK-Sim®.

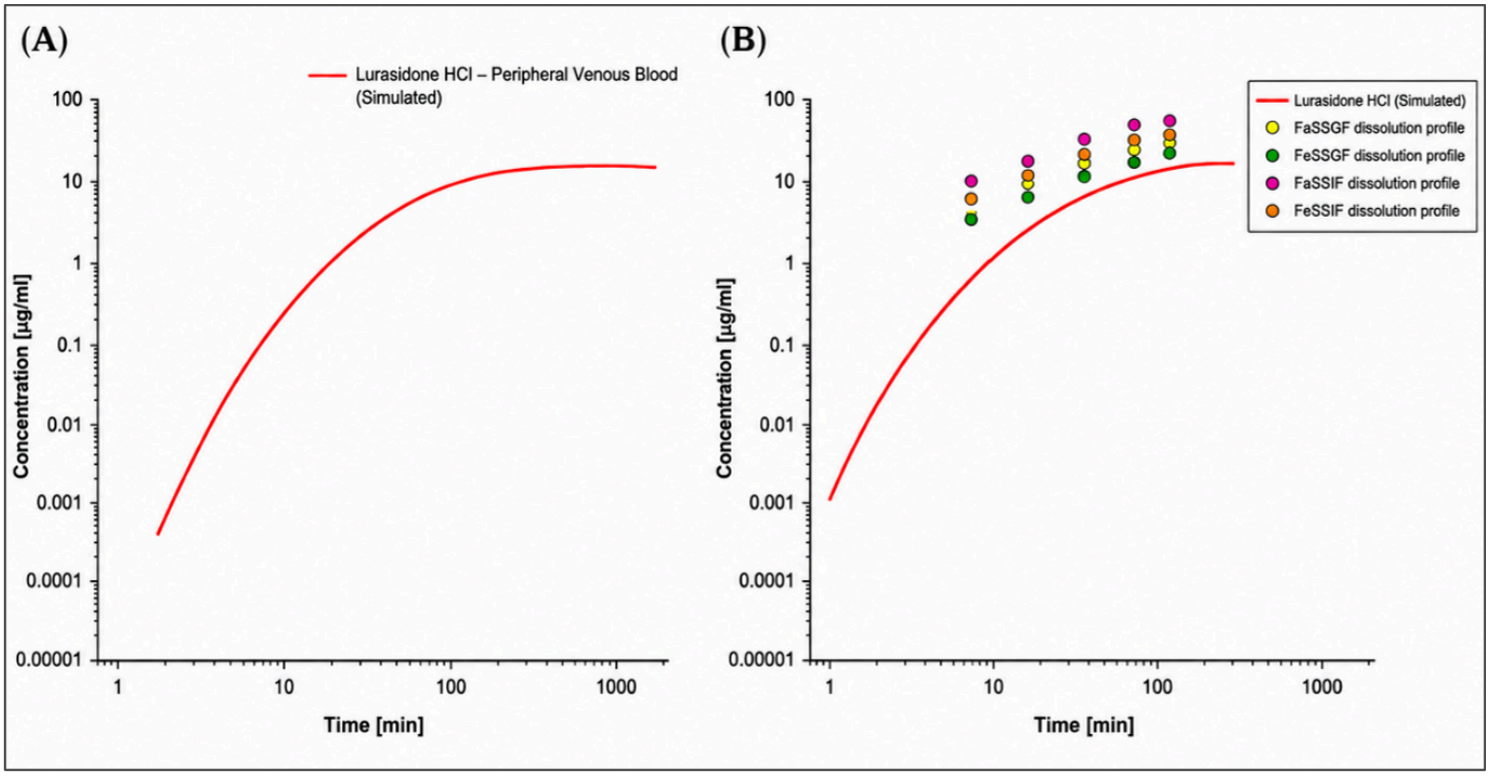


Figure 4

Simulated plasma concentration–time profiles of lurasidone hydrochloride generated using the developed PBPK model under different biorelevant dissolution conditions. (A) Simulated plasma concentration–time profile of lurasidone hydrochloride generated using the developed PBPK model. (B) Comparative simulated plasma concentration–time profiles obtained using dissolution inputs from FaSSGF, FeSSGF, FaSSIF, and FeSSIF.

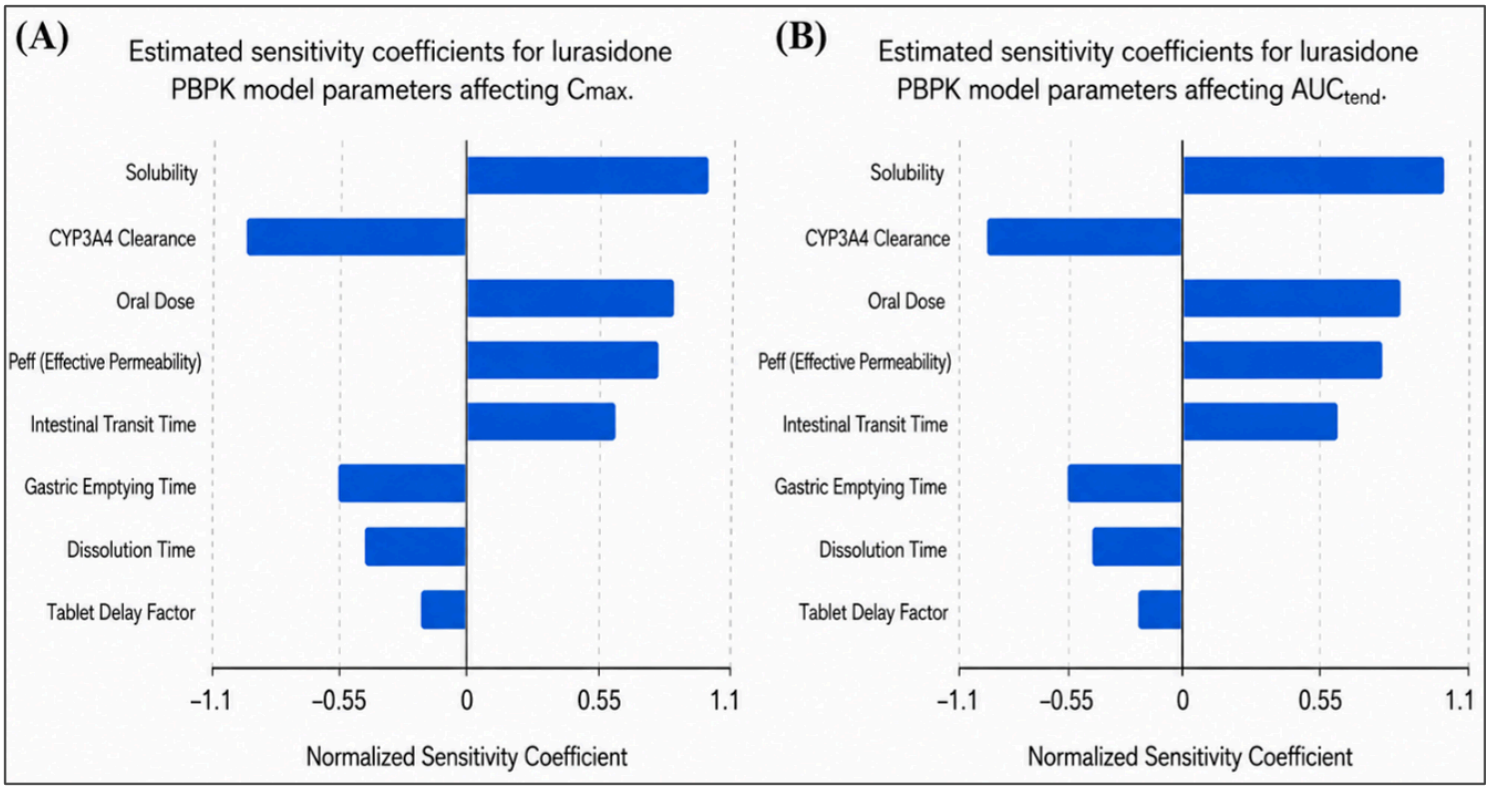


Figure 5

Tornado plots of sensitivity coefficients affecting predicted pharmacokinetic parameters of lurasidone hydrochloride. (A) Sensitivity coefficients influencing predicted maximum plasma concentration (Cmax). (B) Sensitivity coefficients influencing predicted area under the concentration–time curve to the end of the simulation (AUCtend).

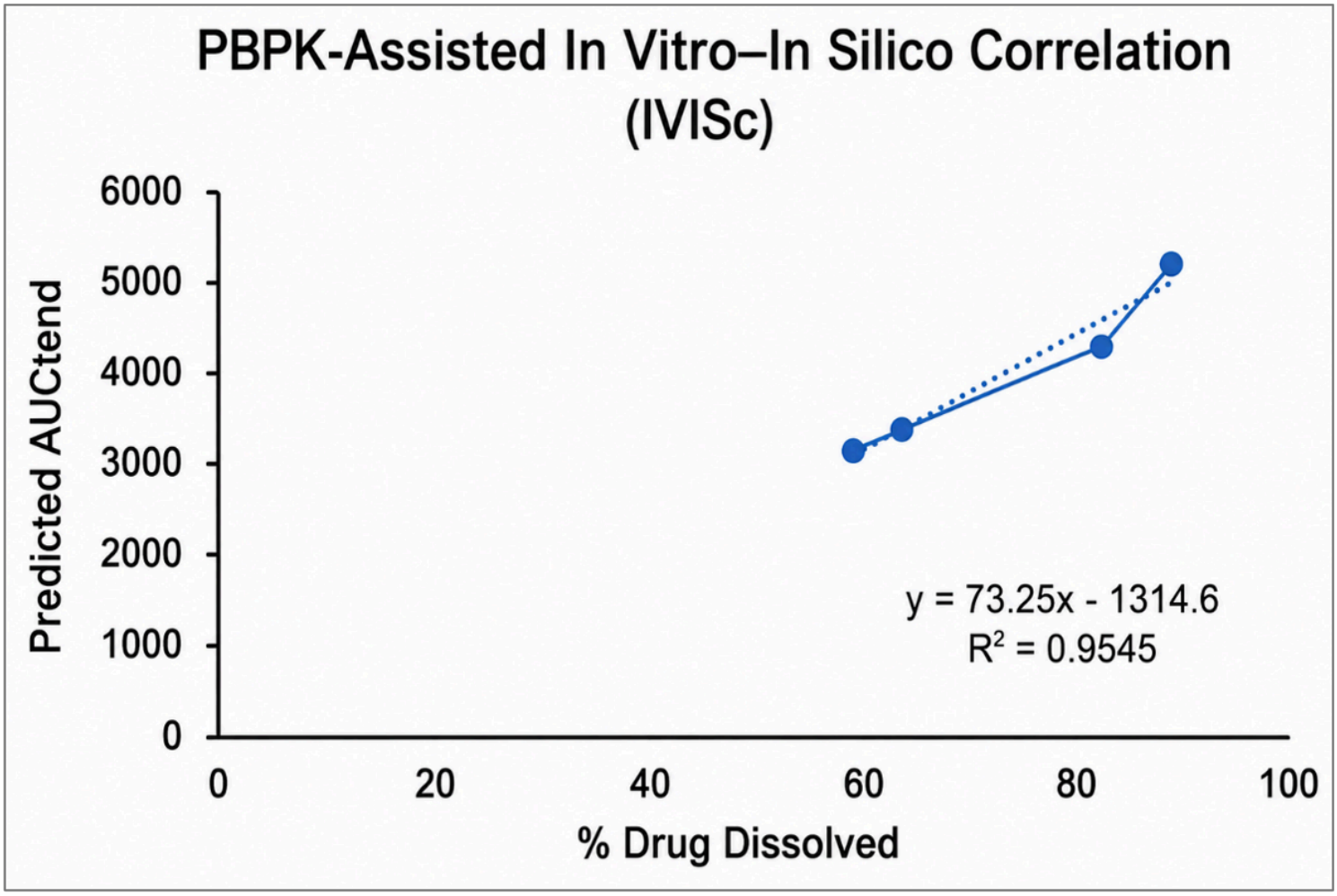


Figure 6

Relationship between percentage drug dissolved at 120 min in biorelevant media and PBPK-predicted AUCtend of lurasidone hydrochloride.

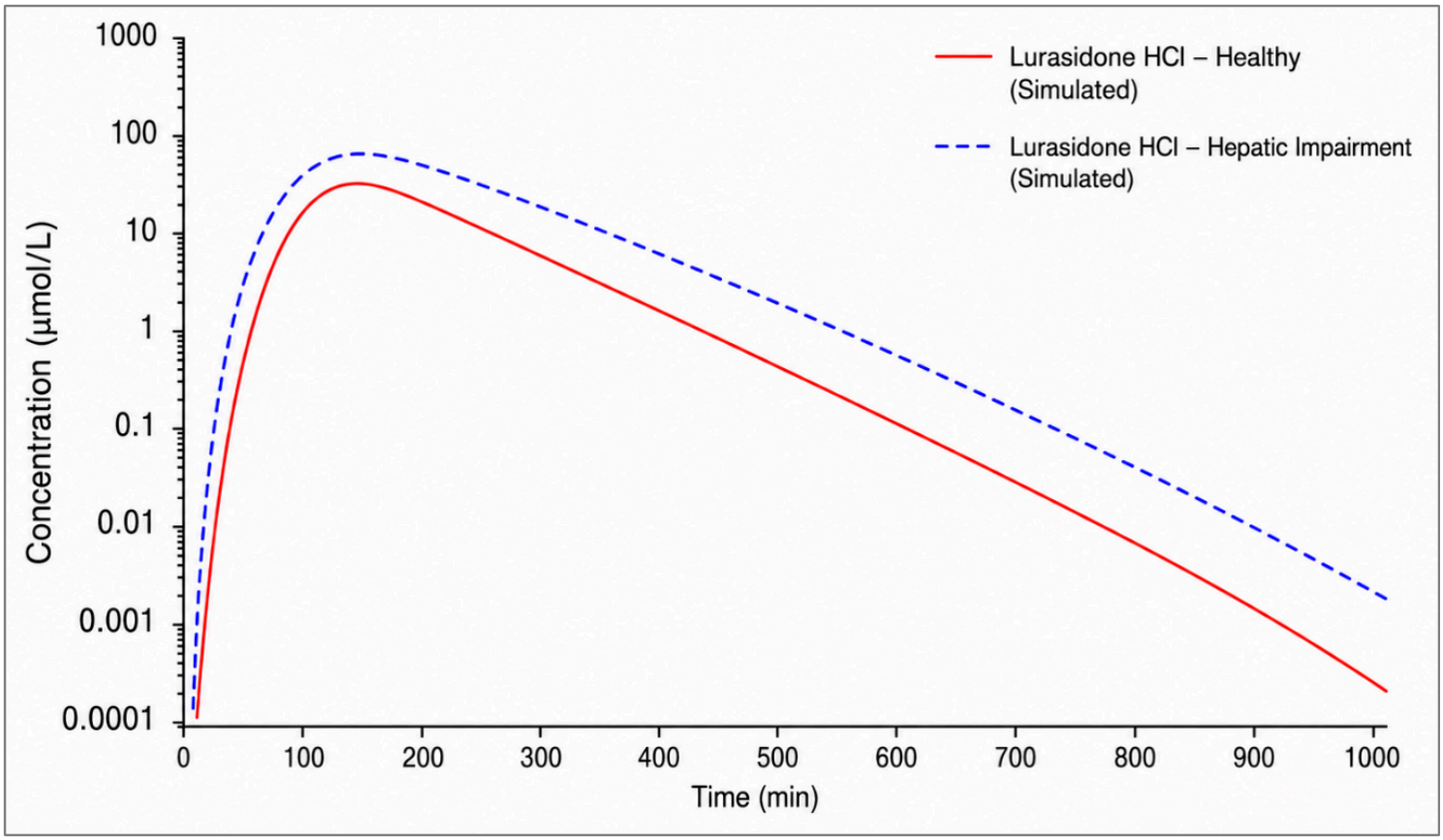


Figure 7

Simulated plasma concentration–time profiles of lurasidone in healthy adults and subjects with hepatic impairment.

Supplementary Files

This is a list of supplementary files associated with this preprint. Click to download.

- SupplementaryInformation.docx